

A Zero-State Coupled Markov Switching Poisson Model for Spatio-temporal Infectious Disease Counts

Dirk Douwes-Schultz* and Alexandra M. Schmidt

*Department of Epidemiology, Biostatistics and Occupational Health
McGill University, Canada*

February 28, 2025

Abstract

Spatio-temporal counts of infectious disease cases often contain an excess of zeros. Existing zero inflated Poisson models applied to such data do not adequately capture the switching of the disease between periods of presence and absence overtime. As an alternative, we develop a new zero-state coupled Markov switching Poisson Model, under which the disease switches between periods of presence and absence in each area through a series of partially hidden nonhomogeneous Markov chains coupled between neighboring locations. When the disease is present, an autoregressive Poisson model generates the cases with a possible 0 representing the disease being undetected. Bayesian inference and prediction is illustrated using spatio-temporal counts of dengue fever cases in Rio de Janeiro, Brazil.

Key words : Bayesian paradigm; Dengue fever; Forward filtering backward sampling; Zero-inflation; Hidden Markov model; State space model

1 Introduction

In epidemiology, counts of infectious disease cases are being increasingly reported in several related areal units across time. A common issue encountered when modeling these counts is the presence of excess zeros (Arab, 2015). That is, there are often many more zeros in the counts than can be predicted by the usual Poisson and negative binomial count models.

*Corresponding author: Dirk Douwes-Schultz, Department of Epidemiology, Biostatistics and Occupational Health, McGill University, 1020 Pine Avenue, Montreal, QC, Canada, H3A 1A2. E-mail: dirk.douwes-schultz@mail.mcgill.ca.

Lambert (1992) proposed the zero inflated Poisson (ZIP) model to deal with excess zeros in count data, and this approach, with various extensions (see Young et al. (2020)), has been applied in many fields including epidemiology. In a disease mapping application of the ZIP model, the presence/absence of the disease is generated through a Bernoulli process and then, when the disease is present, the number of reported cases is generated through a Poisson process (Fernandes et al., 2009). A zero coming from the Poisson process represents the disease being undetected, while a zero from the Bernoulli process represents the true absence of the disease. A ZIP model can help account for the excess zeros, through the additional Bernoulli zero generation, and also allows us to investigate factors related to the presence/absence of the disease while considering imperfect detection of disease presence (Vergne et al., 2016). ZIP models have become increasingly popular in epidemiology for modeling excess zeros in spatio-temporal infectious disease counts (Fernandes et al., 2009; Aktekin and Musal, 2015; Wangdi et al., 2018).

However, in a spatio-temporal setting, existing ZIP approaches do not adequately capture the switching of an infectious disease between periods of presence and absence overtime, for several reasons. Firstly, existing ZIP models only model the probability of overall disease presence. In a spatio-temporal setting we can separate the presence of a disease into two events of epidemiological interest, persistence (presence to presence) and reemergence (absence to presence). Some important epidemiological covariates might affect the reemergence and persistence of an infectious disease quite differently. An example we will give in Section 2 is temperature for dengue fever, as temperature affects both the hatching rate of vertically infected mosquito eggs, which is more important for the reemergence of the disease, and the life cycle of the infected mosquitoes, which is more important for the persistence of the disease (Coutinho et al., 2006). The second issue is that an infectious disease will often switch between long periods of disease presence and long periods of disease absence in an area (Adams and Boots, 2010), while the usual ZIP models can only produce one of these scenarios. This is discussed some by Chen et al. (2019) who point out that the conventional ZIP models cannot account for many consecutive zeros. Actually, they can account for many consecutive zeros just not in conjunction with many consecutive positive counts, which is the usual situation with infectious disease counts. Finally, the inclusion of random effects (e.g. conditional auto regressive CAR (Besag, 1974) effects) in the Bernoulli process of a ZIP model, which are often used to account for spatio-temporal correlations in the presence of the disease (Vergne et al., 2016), can lead to issues in sampling from the posterior distributions due to improper or nearly improper posteriors (Corpas-Burgos et al., 2018). Additionally, temporal prediction is often not possible with improper CAR random effects and the interpretation of the effects is often not useful for policy makers.

To help address these issues we take a zero-state Markov switching approach to modeling the zero inflation. Markov switching models, first introduced by Goldfeld and Quandt (1973) and extensively developed by Hamilton (1989), allow a time series to be described by several submodels (states) where switching between submodels is governed by a first order Markov chain. The motivation behind the Markov switching model, over a finite mixture model, is that the states are often dependent across time and occur consecutively (Goldfeld and Quandt, 1973). Markov switching models that switch between a zero state and a count state were considered in a temporal setting by Wang (2001) and in a spatio-temporal setting by Malyshkina and Mannering (2010). However, Malyshkina and Mannering (2010) assumed the states were independent between spatial units and neither of these applications dealt with infectious disease data.

In our framework, following traditional disease mapping ZIP models (Fernandes et al., 2009), we assume the existence of a zero state, representing the absence of the disease, and a Poisson state, representing the presence of the disease. Then we allow the disease to switch between the presence and absence state in each area through a nonhomogeneous (Diebold et al., 1993) Markov chain. As the disease can spread between areas, we extend the zero-state Markov switching count model to a coupled Markov switching model (Pohle et al., 2020), by coupling the Markov chains between neighboring areas. In a coupled Markov switching model, the transitional probabilities of a Markov chain can depend on the states of other Markov chains. To be more specific, we model the probabilities of disease reemergence and persistence separately, where each probability can depend on covariates, with possibly differing effects, and the, possibly undetected, presence of the disease in neighboring areas. This largely addresses the issues we have discussed with the existing ZIP models, which are mostly nested in the Markov switching model. In particular, the coupled Markov chains allow us to account for spatio-temporal correlations in the presence of the disease without dealing with the issues around the use of random effects in the Bernoulli process (Corpas-Burgos et al., 2018). We can also give useful interpretations about the correlations in disease presence, in terms of consecutiveness in disease presence/absence within an area and the propensity of the disease to spread between areas; and we can provide temporal predictions that account for, possibly undetected, disease presence in the area and neighboring areas. Additionally, a Markov switching model can easily consider both many consecutive zeros and positive counts, as it separates the modeling of having a consecutive zero state and a consecutive count state.

This paper is structured as follows. In Section 1.1 we introduce our motivating example of dengue fever cases in Rio de Janeiro and lay out the goals for our analysis. In Section 2 we introduce our proposed model, the zero-state coupled Markov switching Poisson model.

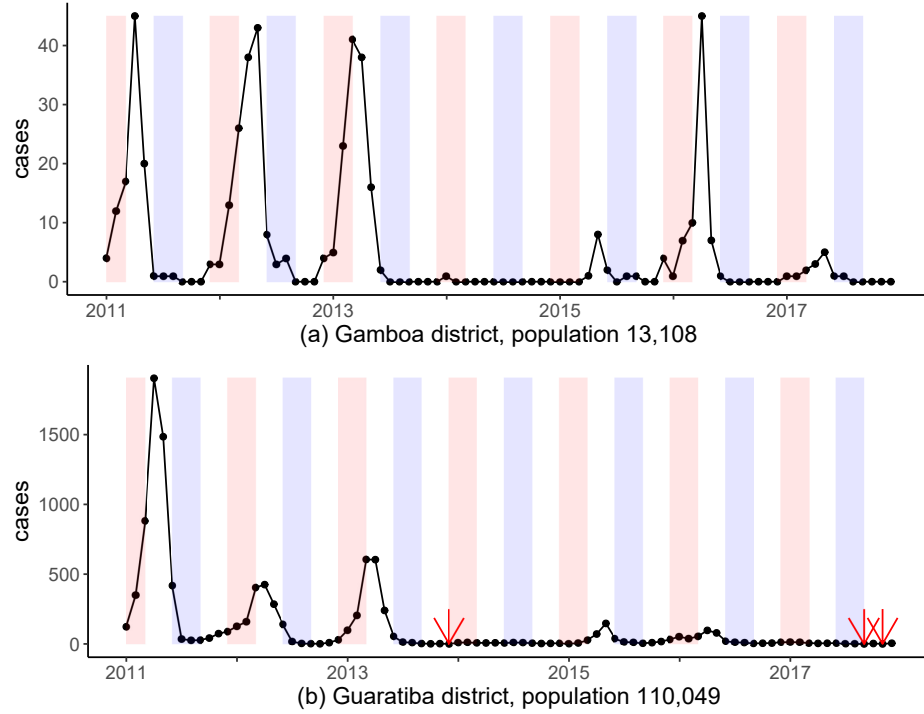


Figure 1: Monthly cases of dengue fever for 2 districts. Summer/winter seasons highlighted in red/blue. In (b), the 3 red arrows point to the only 3 months with 0 cases in this district during the study period.

In Section 3 we describe Bayesian inference using data augmentation through Markov chain Monte Carlo (MCMC) methods. Here we discuss efficient sampling strategies for the parameters and unknown state indicators. In Section 4 we apply the model to the Rio dengue fever data. Finally, we close with a general discussion in Section 5.

1.1 Motivating example: dengue fever in Rio de Janeiro

Dengue fever is endemic in Rio de Janeiro, Brazil, and there have been several major epidemics there since 1987. We focus on modeling monthly cases of dengue fever in the 160 districts of Rio de Janeiro between 2011-2017, as reported by the Health Secretary for the city (<http://www.rio.rj.gov.br/web/sms/exibeconteudo?id=2815389>). Figure 1 shows monthly dengue fever cases for two districts, a relatively small district (a) and relatively large district (b). In the smaller district, there are both long periods of dengue presence (9 months longest period) and long periods of dengue absence (14 months longest period). Additionally, in the smaller district there is clearly a recurring seasonal pattern to the persistence and reemergence of the disease. The disease has a lower chance of persisting during the winter, where it often goes extinct, and then dengue often reemerges in the summer. This

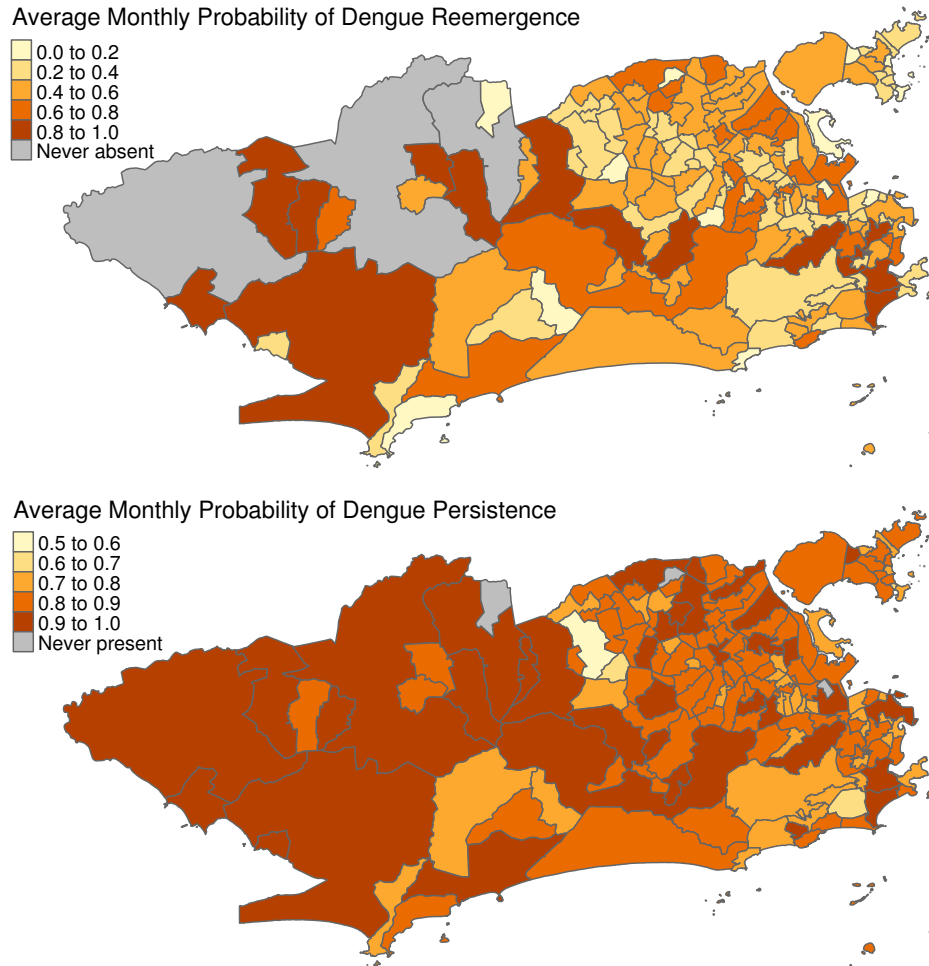


Figure 2: (top) Average monthly probability of dengue reemergence based on reported cases, i.e. $\frac{\#(\text{cases}=0 \rightarrow \text{cases}>0)}{\#(\text{cases}=0 \rightarrow \text{cases}>0) + \#(\text{cases}=0 \rightarrow \text{cases}=0)}$. (bottom) Average monthly probability of dengue persistence based on reported cases, i.e. $\frac{\#(\text{cases}>0 \rightarrow \text{cases}>0)}{\#(\text{cases}>0 \rightarrow \text{cases}>0) + \#(\text{cases}>0 \rightarrow \text{cases}=0)}$.

could be due to changes in rainfall and temperature, which often lead to large fluctuations in the mosquito population (Marquardt, 2004). Additionally, temperature and rainfall play an important role in the life cycle of vertically infected eggs, which are important for the reemergence of the disease (Coutinho et al., 2006). The same patterns in disease presence are not seen in the larger district, where dengue persists for much longer on average compared to the smaller district, rarely goes extinct and reemerges quickly. Figure 2 similarly shows that there is significant spatial variation in the district level average, across time, probabilities of dengue reemergence and persistence (although these are based on reported cases and do not account for imperfect detection of disease presence). This could be explained by differences in population between districts (Bartlett, 1957), but also possibly differences in socioeconomic factors as mosquito's often use human made water containers to lay eggs

(Schmidt et al., 2011).

A statistical model can help quantify some of the above patterns. Specifically, the goal of our analysis is to investigate how certain risk factors (such as rainfall, temperature, socioeconomic factors and population size) are related to the reemergence and persistence of the disease, and when the disease is present, to see how the incidence of dengue changes across time and space. Additionally, as Stoddard et al. (2013) showed that many individuals are infected by dengue outside their homes, we want to quantify the risk of dengue spreading between neighboring districts. Finally, we wish to design some useful warning/forecasting systems for policy makers. As we will explain in the next Section, existing ZIP proposals cannot adequately meet our analysis goals. Specifically, with existing ZIP models we cannot investigate whether a risk factor is affecting the reemergence and persistence of dengue differently, we may not be able to account for the long periods of dengue absence in conjunction with the long periods of dengue presence in the smaller districts, and CAR random effects are hard to interpret in terms of the risk for dengue spreading between areas and may lead to issues with improper posteriors. Therefore, we focus on developing zero-state coupled Markov switching Poisson models which have several advantages over the more traditional ZIP models.

2 A Zero state coupled Markov switching Poisson model

Assume we have areal data with $i = 1, \dots, N$ areas and $t = 1, \dots, T$ time periods. Let y_{it} be the reported case count from area i during time t . Let S_{it} be a binary indicator for the true presence of the disease, meaning $S_{it} = 1$ if the disease is present in area i during time t and $S_{it} = 0$ if the disease is absent. In a Markov switching context, S_{it} represents the state indicator of the model, where $S_{it} = 0$ corresponds to the zero state and $S_{it} = 1$ corresponds to the count state (see (4) below). Let $\mathbf{S}_{(-i)(t-1)} = \{S_{j(t-1)}\}_{j \neq i}$ be the set containing the state indicators of all areas excluding area i at time $t - 1$; and let $\mathbf{y}^{(t-1)} = (\mathbf{y}_1, \dots, \mathbf{y}_{t-1})^T$ be the vector of all case counts up to time $t - 1$, where $\mathbf{y}_t = (y_{1t}, \dots, y_{Nt})^T$.

To model the switching between periods of disease presence and absence in area i , we assume that S_{it} follows a two state nonhomogeneous Markov chain conditional on $\mathbf{S}_{(-i)(t-1)}$ and $\mathbf{y}^{(t-1)}$. We propose the following conditional transition matrix for the Markov chain, for $t = 1, \dots, T$,

$$\Gamma(S_{it} | \mathbf{S}_{(-i)(t-1)}, \mathbf{y}^{(t-1)}) = \begin{array}{c|cc} \text{State} & S_{it}=0 \text{ (absence)} & S_{it}=1 \text{ (presence)} \\ \hline S_{i(t-1)}=0 \text{ (absence)} & 1 - p01_{it} & p01_{it} \\ S_{i(t-1)}=1 \text{ (presence)} & 1 - p11_{it} & p11_{it} \end{array}, \quad (1)$$

where,

$$\begin{aligned} p01_{it} &= P(S_{it} = 1 | S_{i(t-1)} = 0, \mathbf{S}_{(-i)(t-1)}, \mathbf{y}^{(t-1)}) && \text{(probability of disease reemergence)} \\ p11_{it} &= P(S_{it} = 1 | S_{i(t-1)} = 1, \mathbf{S}_{(-i)(t-1)}, \mathbf{y}^{(t-1)}) && \text{(probability of disease persistence).} \end{aligned}$$

The probability of disease reemergence in area i during time t , $p01_{it}$, is allowed to depend on a K -dimensional vector of space-time covariates $\mathbf{z}_{it} = (z_{it1}, \dots, z_{itK})^T$ as well as the number of neighboring areas with the disease present during the previous time period,

$$\text{logit}(p01_{it}) = \zeta_0 + \mathbf{z}_{it}^T \boldsymbol{\zeta} + \zeta_{K+1} \sum_{j \in NE(i)} S_{j(t-1)}, \quad (2)$$

where $NE(i)$ is the set of all neighboring locations of location i . The probability of disease persistence, $p11_{it}$, is defined similarly but all coefficients can differ,

$$\text{logit}(p11_{it}) = \eta_0 + \mathbf{z}_{it}^T \boldsymbol{\eta} + \eta_{K+1} \sum_{j \in NE(i)} S_{j(t-1)}. \quad (3)$$

The transition probabilities can depend on $\mathbf{y}^{(t-1)}$ through \mathbf{z}_{it} , which may contain transformed lagged values of the reported cases (e.g. $\log(y_{i(t-1)} + 1)$). This can be justified by the fact that the disease will only go extinct when there is a small number of infectious individuals. We also need to specify an initial state distribution for the Markov chain in each area, i.e. $p(S_{i0})$ for $i = 1, \dots, N$.

We assume that when the disease is present the cases are generated by a Poisson distribution and that when the disease is absent no cases will be reported, that is,

$$y_{it} | S_{it}, \mathbf{y}^{(t-1)} \sim \begin{cases} 0, & \text{if } S_{it} = 0 \\ \text{Poisson}(\lambda_{it}), & \text{if } S_{it} = 1, \end{cases} \quad (4)$$

where λ_{it} is the expected number of reported cases given the disease is present. The ZIP formulation models imperfect detection of the cases, as a zero generated by the Poisson distribution in (4) represents the disease being undetected and a zero generated through $S_{it} = 0$ represents the *true absence* of the disease. In general we assume the following form for λ_{it} ,

$$\lambda_{it} = g(\boldsymbol{\beta}, \mathbf{x}_{it}, \mathbf{y}^{(t-1)}), \quad (5)$$

where $g(\cdot)$ is some positive valued function, $\boldsymbol{\beta}$ is a vector of unknown parameters (including

possibly random effects) and \mathbf{x}_{it} is a vector of covariates. Therefore, λ_{it} can depend on past values of the case counts, to possibly account for temporal autocorrelation due to transmission of the disease, but not on past values of the state indicators, which is a common assumption in Markov switching models that greatly simplifies model fitting (Frühwirth-Schnatter, 2006).

We will call the model defined by (1)-(5), a zero-state coupled Markov switching Poisson (ZS-CMSP) model. We will now go over the model in detail and explain how it can address many of the issues with existing ZIP models.

The probability the disease will be absent in location i during time t given it was absent at time $t-1$ is given by $1-p01_{it}$. That is, $1-p01_{it}$ is the probability of having a consecutive zero state and, therefore, as $p01_{it}$ approaches 0 consecutive zero counts become more likely. Similarly, $p11_{it}$ is the probability of having a consecutive count state and as $p11_{it}$ approaches 1 consecutive positive counts become more likely. Therefore, the ZS-CMSP model can easily consider many consecutive zeros and/or positive counts in the cases. In contrast, the ZIP model assumes $p01_{it} = p11_{it}$ for all i and t (see below). The issue with this is that we usually observe $p01_{it} << p11_{it}$ empirically, see Figure 2 for example. This can explain the switching between long periods of disease absence and long periods of disease presence that are often seen for infectious diseases in smaller areas, see Figure 1 (a) and Adams and Boots (2010). By restricting $p01_{it} = p11_{it}$ the ZIP model cannot adequately model this scenario as it can only consider many consecutive zeros or positive counts (not both). The consecutiveness in the states can vary across time and space with the ZS-CMSP model, as $p01_{it}$ and $p11_{it}$ can depend on space-time covariates (see (2)-(3)), which makes sense in most applications. For example, with dengue fever there will likely be more longer periods of disease absence during the winter, when mosquitoes are not active, and in smaller districts (Bartlett, 1957).

In the ZS-CMSP model, the effect of covariate z_{itk} on the reemergence of the disease, represented by ζ_k in (2), can be different from its effect on the persistence of the disease, represented by η_k in (3). The advantage of considering differing effects for each covariate on the reemergence and persistence of the disease is that many important epidemiological covariates can interact with the reemergence and persistence of an infectious disease quite differently. For example, a popular theory for dengue reemergence after long periods of disease absence is the hatching of vertically infected mosquito eggs, which hatch due to increases in temperature (Coutinho et al., 2006). This dynamic might not play as much of a role if the disease is already present and other temperature related dynamics might come into play like the life cycle of infected mosquitoes. Therefore, we should investigate whether temperature has a separate effect on the reemergence of dengue compared to the persistence. An additional point in favor of separate space-time covariate effects, at least in

our application, is that there appears, from Figure 2, to be much more spatial variability in the probabilities of dengue reemergence compared to persistence. We will discuss this more in Section 4, and give a possible explanation based on our fitted model.

The $\sum_{j \in NE(i)} S_{j(t-1)}$ terms in (2)-(3) represent the number of neighboring areas with the disease present during the previous time period. From a purely statistical perspective, we are borrowing strength across areas to help determine the states. Note that this neighboring disease presence is only partially observed (e.g. if we observe 0 reported cases in a neighboring area then the disease could be absent or undetected and thus present), however, we can accommodate this, as from a Bayesian point of view, the unknown state indicators become parameters to be estimated (see Section 3). Again, we allow the effect of neighboring disease presence on the reemergence of the disease to be different from its effect on the persistence of the disease. The disease may spread to non-infected areas from neighboring areas (modeled through ζ_{K+1} in (2)); but also, neighboring areas can supply infectious individuals needed to maintain the persistence of the disease in infected areas (modeled through η_{K+1} in (3)) (Okano et al., 2020). The effects of these two traveling dynamics on the presence of the disease may differ. Our way of modeling spatial correlation in the presence of the disease avoids issues with improper posteriors that can arise when using CAR random effects in the Bernoulli process of a ZIP model (Corpas-Burgos et al., 2018). Indeed, many authors have reported Bayesian convergence issues when using these random effects in the Bernoulli process (Aktekin and Musal, 2015), which could be a manifestation of the issues described by Corpas-Burgos et al. (2018). Another advantage of coupling is that the interpretation about the spatial correlations is straightforward and gives the risk for the disease to spread from neighboring areas, which can be useful for policy makers. Additionally, temporal prediction is intuitive with the ZS-CMSP model (see Section 3.1), while prediction is often not possible when using improper CAR random effects.

Clearly, the ZS-CMSP model addresses the many issues with the ZIP model that arise in a spatio-temporal setting. In fact, the ZIP model of Lambert (1992) is nested within the ZS-CMSP model which reduces to it when $\zeta_0 = \eta_0$, $\boldsymbol{\zeta} = \boldsymbol{\eta}$ and $\zeta_{K+1} = \eta_{K+1} = 0$. Therefore, the ZIP model assumes that the effect of each covariate on the reemergence of the disease is the same as its effect on the persistence, that the average probability of disease reemergence is the same as the average probability of disease persistence and it does not directly consider neighboring disease presence (random effects can be added to the Bernoulli process which comes with the issues described previously). This is the same as assuming $p01_{it} = p11_{it}$ for all i and t , and that $\zeta_{K+1} = \eta_{K+1} = 0$. In the supplementary material (SM) section 2, we include a simulation study that shows the ZIP model can be recovered when fitting the ZS-CMSP model, meaning the credible intervals of the Markov chain parameters can be

used to help asses if the ZIP model is more appropriate.

We make the following conditional independence assumptions, $S_{it} \perp\!\!\!\perp S_{jt} \mid (\mathbf{S}_{t-1}, \mathbf{y}^{(t-1)})$, $y_{it} \perp\!\!\!\perp y_{jt} \mid (\mathbf{S}_t, \boldsymbol{\beta}, \mathbf{y}^{(t-1)})$, for all $i \neq j$ and $t = 1, \dots, T$, and we similarly assume $S_{i0} \perp\!\!\!\perp S_{j0}$ for all $i \neq j$. Without these assumptions it is difficult to construct the likelihood function (Spezia et al., 2017), however, in a disease mapping setting these are reasonable assumptions. The first assumption states that the disease spreads between areas in a lagged manner. This is a common assumption in infectious disease modeling and is often reasonable considering delays between infection and secondary cases (Bauer and Wakefield, 2018).

Let $\mathbf{S}_t = (S_{1t}, \dots, S_{Nt})^T$ be the set of all state indicators at time t . \mathbf{S}_t forms a first order Markov chain, conditional on $\mathbf{y}^{(t-1)}$, with state space $\{0, 1\}^N$ and $2^N \times 2^N$ transition matrix $\Gamma(\mathbf{S}_t | \mathbf{y}^{(t-1)})$. An element of $\Gamma(\mathbf{S}_t | \mathbf{y}^{(t-1)})$ is given by,

$$\begin{aligned} P\left(S_{1t} = s_{1t}, \dots, S_{Nt} = s_{Nt} \mid S_{1(t-1)} = s_{1(t-1)}, \dots, S_{N(t-1)} = s_{N(t-1)}, \mathbf{y}^{(t-1)}\right) \\ = \prod_{i=1}^N P\left(S_{it} = s_{it} \mid \mathbf{S}_{t-1} = \mathbf{s}_{t-1}, \mathbf{y}^{(t-1)}\right). \end{aligned} \quad (6)$$

Therefore, rewriting the ZS-CMSP model in terms of $\Gamma(\mathbf{S}_t | \mathbf{y}^{(t-1)})$ and $p(\mathbf{y}_t | \mathbf{S}_t, \mathbf{y}^{(t-1)}) = \prod_{i=1}^N p(y_{it} | S_{it}, \mathbf{y}^{(t-1)})$ shows that it is a Markov switching model as defined by Frühwirth-Schnatter (2006). However, the transition matrix has an exceptionally large dimension ($2^N \times 2^N$) which creates some issues in inference, as we will discuss next.

3 Inferential Procedure

Let $\mathbf{S} = \{\mathbf{S}_t\}_{t=0}^T$ be the set of all state indicators. A major point in inference is that S_{it} is not observed when $y_{it} = 0$, as a 0 may arise from either the Poisson process or directly from the Markov chain through $S_{it} = 0$. An epidemiological explanation is that if we observe zero reported cases in an area then we do not know if the disease is truly absent or present and undetected. This also arises in other applications. For example, in accident analysis it is not clear if zero reported accidents for a highway segment signals the segment is safe or is due to random chance (Malyshkina and Mannerling, 2010).

The likelihood of $\mathbf{v} = (\boldsymbol{\theta}, \boldsymbol{\beta})^T$, where $\boldsymbol{\theta} = (\zeta_0, \eta_0, \boldsymbol{\zeta}, \boldsymbol{\eta}, \zeta_{K+1}, \eta_{K+1})^T$, given $\mathbf{y} = \{\mathbf{y}_t\}_{t=1}^T$ and \mathbf{S} is given by,

$$L(\mathbf{y}, \mathbf{S} | \mathbf{v}) = \prod_{i=1}^N \prod_{t=1}^T p(y_{it} | S_{it}, \mathbf{y}^{(t-1)}, \boldsymbol{\beta}) \prod_{i=1}^N p(S_{i0}) \prod_{t=1}^T p(S_{it} | \mathbf{S}_{t-1}, \mathbf{y}^{(t-1)}, \boldsymbol{\theta}). \quad (7)$$

When N is large it is not possible to marginalize out \mathbf{S} from (7), as doing so requires matrix multiplication with $\Gamma(\mathbf{S}_t|\mathbf{y}^{(t-1)})$ (Frühwirth-Schnatter, 2006). Therefore, we estimate the unknown elements of \mathbf{S} along with \mathbf{v} by sampling both from their joint posterior distribution which, from Bayes' theorem, is proportional to,

$$p(\mathbf{S}, \mathbf{v}|\mathbf{y}) \propto L(\mathbf{y}, \mathbf{S}|\mathbf{v})p(\mathbf{v}), \quad (8)$$

where $p(\mathbf{v})$ is the prior distribution of \mathbf{v} . We specify independent uninformative normal and gamma priors for all low-level parameters. As the joint posterior is not available in closed form, we resort to Markov chain Monte Carlo methods, in particular, we used a hybrid Gibbs sampling algorithm with some steps of the Metropolis-Hastings algorithm to sample from it. We sampled most elements of \mathbf{v} individually, using an adaptive random walk Metropolis step (Shaby and Wells, 2010). The parameter vectors $(\eta_0, \eta_{K+1})^T$ and $(\zeta_0, \zeta_{K+1})^T$ showed high posterior correlations and, therefore, we jointly sampled them using a blocked adaptive random walk Metropolis step (Roberts and Sahu, 1997). This doubled the efficiency (minimum effective sample size per hour) of the Gibbs sampler in our application.

It is straightforward to sample each unknown element of \mathbf{S} one at a time. When $y_{it} = 0$, the full conditional of S_{it} is given by,

$$\begin{aligned} P(S_{it} = 1|\mathbf{y}, \mathbf{v}, \{S_{jt}\}_{j \neq i, t \in \{0, \dots, T\}}) \\ = \frac{P(y_{it} = 0|S_{it} = 1)P(S_{it} = 1|\mathbf{S}_{t-1})\prod_{j=1}^N p(S_{j(t+1)}|S_{it} = 1, \mathbf{S}_{(-i)(t)})}{\sum_{s_{it}=0}^1 P(y_{it} = 0|S_{it} = s_{it})P(S_{it} = s_{it}|\mathbf{S}_{t-1})\prod_{j=1}^N p(S_{j(t+1)}|S_{it} = s_{it}, \mathbf{S}_{(-i)(t)})}, \end{aligned} \quad (9)$$

where $P(y_{it} = 0|S_{it} = s_{it}) = \exp(-\lambda_{it}s_{it})$ and the dependence of the densities on $\mathbf{y}^{(t-1)}$, $\boldsymbol{\beta}$ and $\boldsymbol{\theta}$ are suppressed to reduce the size of the equation. However, one at a time sampling is known to lead to poor mixing in the Markov switching literature due to the strong posterior correlations between the unknown state indicators (Scott, 2002). Better mixing can be achieved by sampling all of \mathbf{S} jointly from $p(\mathbf{S}|\mathbf{y}, \mathbf{v})$ (Chib, 1996). However, this is not computationally feasible with our model when N is large, as it again involves matrix multiplication with $\Gamma(\mathbf{S}_t|\mathbf{y}^{(t-1)})$ (Frühwirth-Schnatter, 2006). As an alternative, we propose to block sample \mathbf{S} with each block containing all the state indicators in a different collection of locations. More specifically, assume we have put the locations into $c = 1, \dots, C$ blocks with n_c locations in block c and that $\sum_{c=1}^C n_c = N$. Let $\mathbf{S}_{(c)}$ be the set of all state indicators in block c and let $\mathbf{S}_{(-c)}$ be the set of all state indicators outside of block c . The idea is to

jointly sample $\mathbf{S}_{(c)}$ from its full conditional distribution, given by,

$$\begin{aligned} p(\mathbf{S}_{(c)} | \mathbf{S}_{(-c)}, \mathbf{y}, \mathbf{v}) &= p(\mathbf{S}_{(c)\mathbf{T}} | \mathbf{S}_{(-c)(0:\mathbf{T})}, \mathbf{y}, \mathbf{v}) \\ &\times \prod_{t=0}^{T-1} p(\mathbf{S}_{(c)t} | \mathbf{S}_{(c)t+1}, \mathbf{S}_{(-c)(0:t+1)}, \mathbf{y}_{(1:N)(1:t)}, \mathbf{v}). \end{aligned} \quad (10)$$

A blocked forward filtering backward sampling (bFFBS) algorithm is needed to sample from (10), which we provide in the SM Section 2. The bFFBS algorithm only requires matrix multiplication with a $2^{n_c} \times 2^{n_c}$ matrix. Our algorithm can be seen as an extension of the individual forward filtering backward sampling (iFFBS) algorithm recently proposed by Touloupou et al. (2020), who considered $n_c = 1$ for all c .

Our hybrid Gibbs sampler was implemented using the R package Nimble (de Valpine et al., 2017). Nimble comes with built in Metropolis-Hastings, blocked Metropolis-Hastings and binary (equivalent to one at a time sampling for the unknown presence/absence indicators) samplers. The bFFBS samplers were implemented using Nimble's custom sampler feature. All Nimble R code, including for the custom bFFBS samplers, are provided in the supplementary material (https://github.com/Dirk-Douwes-Schultz/ZS_CMSP_code). Nimble was chosen as it is extremely fast (C++ compiled) and only requires the coding of new samplers. In the SM Section 2, we provide a simulation study which shows that our proposed Gibbs sampler can recover the true parameters of the ZS-CMSP model.

3.1 Temporal Prediction

We will assume only dependence on counts from the immediately preceding time for simplicity in notation. We can use Monte Carlo integration (see SM Section 3 for details) to approximate the one step ahead posterior predictive distribution of disease presence in location i ,

$$P(S_{i(T+1)} = 1 | \mathbf{y}) \approx \frac{1}{Q - M} \sum_{m=M+1}^Q P(S_{i(T+1)} = 1 | S_{iT}^{[m]}, \mathbf{S}_{(-i)\mathbf{T}}^{[m]}, \mathbf{y}_{\mathbf{T}}, \boldsymbol{\theta}^{[m]}), \quad (11)$$

for $i = 1, \dots, N$, where the superscript $[m]$ denotes a draw from the posterior distribution of the parameter, M is the size of the burn-in sample and Q is the total MCMC sample size. We can similarly approximate the one step ahead posterior predictive distribution of

the cases in location i ,

$$p(y_{i(T+1)}|\mathbf{y}) \approx \frac{1}{Q-M} \sum_{m=M+1}^Q \left[p(y_{i(T+1)}|S_{i(T+1)} = 1, \mathbf{y}_T, \boldsymbol{\beta}^{[m]}) P(S_{i(T+1)} = 1|S_{iT}^{[m]}, \mathbf{S}_{(-i)T}^{[m]}, \mathbf{y}_T, \boldsymbol{\theta}^{[m]}) \right. \\ \left. + I[y_{i(T+1)} = 0] \left(1 - P(S_{i(T+1)} = 1|S_{iT}^{[m]}, \mathbf{S}_{(-i)T}^{[m]}, \mathbf{y}_T, \boldsymbol{\theta}^{[m]}) \right) \right], \quad (12)$$

for $i = 1, \dots, N$, where $I[\cdot]$ is an indicator function. Therefore, the one step ahead posterior predictive distribution of the counts is zero inflated, where the mixing probability depends on past histories of the states and counts. We can expand (11) to gain a better understanding of this one step ahead prediction for the risk of disease presence in location i ,

$$P(S_{i(T+1)} = 1|S_{iT}^{[m]}, \mathbf{S}_{(-i)(T)}^{[m]}, \mathbf{y}_T, \boldsymbol{\theta}^{[m]}) = p01_{i(T+1)}^{[m]}(1 - S_{iT}^{[m]}) + p11_{i(T+1)}^{[m]}S_{iT}^{[m]}, \text{ where,} \\ \text{logit}(p01_{i(T+1)}^{[m]}) = \zeta_0^{[m]} + \mathbf{z}_{i(T+1)}^T \boldsymbol{\zeta}^{[m]} + \zeta_{K+1}^{[m]} \sum_{j \in NE(i)} S_{jT}^{[m]} \\ \text{logit}(p11_{i(T+1)}^{[m]}) = \eta_0^{[m]} + \mathbf{z}_{i(T+1)}^T \boldsymbol{\eta}^{[m]} + \eta_{K+1}^{[m]} \sum_{j \in NE(i)} S_{jT}^{[m]}. \quad (13)$$

Even if for $j \in NE(i)$ $y_{jT} = 0$, $S_{jT}^{[m]}$ could be 1 for many m if there is a high chance the disease went undetected in neighbor j . Similarly, if $y_{iT} = 0$, $S_{iT}^{[m]}$ could be 1 for many m if there is a high chance the disease is undetected in location i . Therefore, this warning system accounts for the fact that the disease may already have been circulating undetected in location i for some time. It also considers the possible risk of spread from neighboring locations with 0 reported cases that have a high chance of the disease being undetected. More traditional warning systems, based on autoregressive models (Chan et al., 2015), cannot account for these important risks. This makes our warning system particularly useful in cities like Rio where underreporting is a major issue, and the disease may circulate and spread unnoticed.

For arbitrary K step ahead predictions, we use a simulation procedure (Frühwirth-Schnatter, 2006) to draw samples from the posterior predictive distributions. Algorithm 1 will obtain realizations from the posterior predictive distribution of the cases, $y_{i(T+k)}^{[m]} \sim p(y_{i(T+k)}|\mathbf{y})$, and the presence of the disease, $S_{i(T+k)}^{[m]} \sim p(S_{i(T+k)}|\mathbf{y})$, for $i = 1, \dots, N$ and $k = 1, \dots, K$. However, as $S_{i(T+k)}^{[m]}$ can only take two values, 0 or 1, it is difficult to interpret the uncertainty around this prediction for the presence of the disease. Therefore, instead of using summaries of $S_{i(T+k)}^{[m]}$ we use summaries of $P(S_{i(T+k)} = 1|S_{i(T+k-1)}^{[m]}, \mathbf{S}_{(-i)(T+k-1)}^{[m]}, \mathbf{y}_{T+k-1}^{[m]}, \boldsymbol{\theta}^{[m]})$.

Algorithm 1: Posterior Predictive Simulation

```

for  $m$  in  $M + 1 : Q$  do
  for  $k$  in  $1 : K$  do
    for  $i$  in  $1 : N$  do
      1. Draw  $S_{i(T+k)}^{[m]}$  from  $p(S_{i(T+k)} | S_{T+k-1}^{[m]}, \mathbf{y}_{T+k-1}^{[m]}, \boldsymbol{\theta}^{[m]})$ , where  $\mathbf{y}_T^{[m]} = \mathbf{y}_T$ ,
          $p(S_{i(T+k)} | S_{T+k-1}^{[m]}, \mathbf{y}_{T+k-1}^{[m]}, \boldsymbol{\theta}^{[m]}) = \text{Bern}\left(\pi_{i(T+k)}^{[m]}\right)$ , where,
          $\pi_{i(T+k)}^{[m]} = p01_{i(T+k)}^{[m]}(1 - S_{i(T+k-1)}^{[m]}) + p11_{i(T+k)}^{[m]}S_{i(T+k-1)}^{[m]}$ .
      2. Draw  $y_{i(T+k)}^{[m]}$  from  $p(y_{i(T+k)} | S_{i(T+k)}^{[m]}, \mathbf{y}_{T+k-1}^{[m]}, \boldsymbol{\beta}^{[m]})$ , where  $\mathbf{y}_T^{[m]} = \mathbf{y}_T$ ,
          $p(y_{i(T+k)} | S_{i(T+k)}^{[m]}, \mathbf{y}_{T+k-1}^{[m]}, \boldsymbol{\beta}^{[m]}) = \text{Poisson}(S_{i(T+k)}^{[m]} \lambda_{i(T+k)}^{[m]})$ .
    end
  end
end
  
```

3.2 Fitted Values

Comparing the predictions, for a fixed K , to the observed values is not practical, as it requires fitting the model to multiple time points. This would result in long computational times, with MCMC methods, and unstable estimates for earlier times. Assume in this section $t \in \{1, \dots, T\}$ and $i \in \{1, \dots, N\}$. There are three types of fitted values for a Markov switching model: one step ahead, filtered and smoothed (Hamilton, 1993). In our Bayesian setting, the smoothed fitted values are given by,

$$S_{it}^{*[m]} = S_{it}^{[m]} \text{ drawn from } p(S_{it} | \mathbf{y}), \quad (14)$$

$$y_{it}^{*[m]} \text{ drawn from } p(y_{it} | S_{it}^{[m]}, \mathbf{y}^{(t-1)}, \boldsymbol{\beta}^{[m]}), \quad (15)$$

for $m = M + 1, \dots, Q$. Note, $y_{it}^{*[m]} \sim p(y_{it}^* | \mathbf{y})$, where $y_{it}^* | S_{it}, \mathbf{y}^{(t-1)}, \boldsymbol{\beta} \sim \text{Poisson}(S_{it} \lambda_{it})$. That is, y_{it}^* represents a new case count generated by the same parameters, state and past counts that generated y_{it} . The smoothed fitted value of the state is drawn automatically by the Gibbs sampler used to fit the model, which is an advantage in using data augmentation to fit a Markov switching model. Note that $P(S_{it} = 1 | \mathbf{y}) \approx \frac{1}{Q-M} \sum_{m=M+1}^Q S_{it}^{[m]}$. When $y_{it} = 0$, the $P(S_{it} = 1 | \mathbf{y})$ represents the posterior probability the disease is present and thus undetected. Therefore, a map of the posterior mean of S_{it} for i where $y_{it} = 0$ can be used by policy makers as a warning system to identify areas reporting 0 cases that have a high chance of the disease being undetected.

Clearly, smoothed fitted values represent fits given all information in the data about the

states, including from present and future counts. If the model is not good at predicting the state one step ahead, which is largely based on the estimated transition probabilities of the Markov chain, then the smoothed fitted values may not reveal that as much of the information about S_{it} can come from y_{it} . The one step ahead distribution of the states is given by, $p(\mathbf{S}_t | \mathbf{y}^{(t-1)}, \mathbf{v})$, and of the cases is given by, $p(\mathbf{y}_t | \mathbf{y}^{(t-1)}, \mathbf{v}) = \sum_{s_t \in \{0,1\}^N} p(\mathbf{y}_t | \mathbf{S}_t = s_t, \mathbf{y}^{(t-1)}, \boldsymbol{\beta}) P(\mathbf{S}_t = s_t | \mathbf{y}^{(t-1)}, \mathbf{v})$ (Frühwirth-Schnatter, 2006). As \mathbf{v} is unknown, we can draw from the posterior of the one step ahead distributions. That is, the one step ahead fitted value of the state is given by, $S_{it}^{1*[m]}$ drawn from $p(\mathbf{S}_t | \mathbf{y}^{(t-1)}, \mathbf{v}^{[m]})$, and of the counts is given by, $y_{it}^{1*[m]}$ drawn from $p(y_{it} | S_{it}^{1*[m]}, \mathbf{y}^{(t-1)}, \boldsymbol{\beta}^{[m]})$, for $m = M+1, \dots, Q$, where we use the superscript $1*[m]$ to denote a draw from the posterior of the one step ahead distributions. The advantage of the one step ahead fitted values is that information from $(\mathbf{y}_t, \dots, \mathbf{y}_T)^T$ is only used to learn about \mathbf{v} and not the states. Therefore, they should more accurately reflect the predictions than the smoothed values and should be able to diagnosis a lack of fit in the Markov chain component of the model. The distribution $p(\mathbf{S}_t | \mathbf{y}^{(t-1)}, \mathbf{v}^{[m]})$ can be calculated using a Hamiltonian forward filter (Frühwirth-Schnatter, 2006). However, the filter requires matrix multiplication with $\Gamma(\mathbf{S}_t | \mathbf{y}^{(t-1)})$ and so is not computationally feasible to run when N is large.

As an alternative for large N , we propose coupled one step ahead fitted values. Assume we wish to calculate the one step ahead fitted values for location i when N is large. We will put i in a location block c with neighboring locations. Then, borrowing notation from (10), the coupled one step ahead fitted values are given by,

$$S_{it}^{c1*[m]} \text{ drawn from } p(S_{it} | \mathbf{S}_{(-c)(0:t)}^{[m]}, \mathbf{y}^{(t-1)}, \mathbf{v}^{[m]}), \quad (16)$$

$$y_{it}^{c1*[m]} \text{ drawn from } p(y_{it} | S_{it}^{c1*[m]}, \mathbf{y}^{(t-1)}, \boldsymbol{\beta}^{[m]}), \quad (17)$$

for $m = M+1, \dots, Q$, where we use the superscript $c1*[m]$ to denote a draw from the posterior of the coupled one step ahead distributions. The distribution $P(S_{it} = 1 | \mathbf{S}_{(-c)(0:t)}^{[m]}, \mathbf{y}^{(t-1)}, \mathbf{v}^{[m]})$ can be calculated using the forward filtering part of the bFFBS algorithm given in the supplementary material. We do not use quantiles of $S_{it}^{c1*[m]}$ as it can only take the two values 0 or 1. Instead we use quantiles of $P(S_{it} = 1 | \mathbf{S}_{(-c)(0:t)}^{[m]}, \mathbf{y}^{(t-1)}, \mathbf{v}^{[m]})$, which represents a draw from the posterior distribution of the coupled one step ahead fitted probability of disease presence. We only use information from $(\mathbf{y}_t, \dots, \mathbf{y}_T)^T$ to learn about $\mathbf{S}_{(-c)(0:t)}$. Therefore, if we block neighboring locations together there should be minimal information from $(\mathbf{y}_t, \dots, \mathbf{y}_T)^T$ used in the state estimation.

4 Analysis of the dengue fever data in Rio de Janeiro

4.1 Model Specification and Fitting

The ZS-CMSP model has two components, a nonhomogeneous Markov chain which switches dengue between periods of presence and absence through modeling the reemergence and persistence of the disease, and a Poisson component that generates the reported cases when dengue is present. For the Poisson component, we use an endemic/epidemic specification for λ_{it} (Bauer and Wakefield, 2018), as it can account for temporal autocorrelation due to the onward transmission of the disease,

$$\lambda_{it} = \lambda_{it}^{AR} y_{i(t-1)} + \lambda_{it}^{EN}. \quad (18)$$

The auto regressive rate λ_{it}^{AR} is meant to represent the transmission intensity of dengue in district i during month t . We model λ_{it}^{AR} as, $\log(\lambda_{it}^{AR}) = \beta_{0i}^{AR} + \beta_1 \text{Rain}_{t-1} + \beta_2 \text{Temp}_{t-1}$, where Temp_{t-1} is the maximum temperature in Rio during the previous month, Rain_{t-1} is the millimeters of rainfall and $\beta_{0i}^{AR} \sim N(\beta_0^{AR}, \sigma_{AR})$ are random intercepts accounting for between district differences in transmission intensity, where σ_{AR} is the standard deviation of the random effects. Rainfall and temperature are entered in a lagged manner since there is usually a delay separating changes in mosquito population and dengue incidence (Coutinho et al., 2006). The endemic risk λ_{it}^{EN} accounts for incidence not due to within area transmission. We compared both space-time and space varying endemic risk using the widely applicable information criterion (WAIC) (Gelman et al., 2014) (results not shown) and settled on a purely spatial varying risk, $\log(\lambda_{it}^{EN}) = \beta_{0i}^{EN}$, where $\beta_{0i}^{EN} \sim N(\beta_0^{EN}, \sigma_{EN})$. We considered $\mathbf{z}_{it} = (\text{pop}_i, \text{HDI}_i, \text{Rain}_{t-1}, \text{Temp}_{t-1}, \log(y_{i(t-1)} + 1))^T$, where pop_i is the population of district i and HDI_i is the human development index of district i , as covariates possibly affecting the reemergence and persistence (see equations (2) and (3)) of dengue. Since we condition on the first observation, we specified $p(S_{i1}) \sim \text{Bern}(.5)$ if $y_{i1} = 0$ and $p(S_{i1})$ is degenerate 1 if $y_{i1} > 0$, as the initial state distributions. The monthly rainfall and temperature data were obtained from the National Institute for Space Research (<http://bancodedados.cptec.inpe.br/>) and the district level human development indexes were obtained from ipeadata (<http://www.ipeadata.gov.br/Default.aspx>).

We fit the ZS-CMSP model specified above, using our proposed Gibbs sampler from Section 3, to the monthly Rio dengue cases for 2011-2017 ($t = 1, \dots, 84$) and all districts in the city ($i = 1, \dots, 160$). We ran the Gibbs sampler for 30,000 iterations on 3 chains with a initial burn in of 10,000 iterations. All sampling was started from random values in the parameter space to avoid convergence to local modes. Convergence was checked using

Table 1: Model comparison using WAIC for 3 models fitted to the dengue data.

Model	WAIC
endemic/epidemic	98,046
ZIP	90,640
ZS-CMSP	90,458

the Gelman-Rubin statistic (all estimated parameters <1.05) and the minimum effective sample size (>1000) (Plummer et al., 2006). We compared the efficiency (minimum effective sample size per hour) of 3 candidate samplers for the state indicators: a one at time sampler (binary) and two bFFBS samplers with block sizes 1 (iFFBS) and 2 (bFFBS2). For the bFFBS2 sampler, we blocked 71 neighboring locations together leaving 15 locations that could not be matched to a neighbor that were put in single location blocks (remaining 3 locations had all positive observations and did not need to be sampled). The iFFBS sampler was 10% more efficient than the binary sampler and the bFFBS2 sampler was 16% more efficient. These efficiency gains are smaller than ones found in other studies that jointly sampled the state indicators in a coupled Markov switching model (Touloupou et al., 2020). This could be due to the Markov chain being only partially hidden in the ZS-CMSP model.

We compared the fit of 3 models fitted to the dengue data using WAIC, see Table 1: a model with no zero inflation (endemic/epidemic); a nested ZIP model with $\zeta_0 = \eta_0$, $\zeta = \eta$ and $\zeta_{K+1} = \eta_{K+1} = 0$ (see Section 2); and the ZS-CMSP model. The incorporation of zero inflation significantly improves the fit of the endemic/epidemic model, while the ZS-CMSP model is the superior model for the zero inflation.

The estimated coefficients for the Markov chain part of the fitted ZS-CMSP model are given in Table 2. From the estimated intercepts, consecutive periods of disease presence are heavily favored on average, while consecutive periods of disease absence are only slightly favored on average. This highlights the importance of preventing dengue reemergence, as when the disease does reemerge it will likely persist for some time in an average district. Dengue has, on average, twice the risk of being present if it was present in the previous month. This indicates a strong Markov property and high temporal correlation in disease presence within an area. Population size has a significantly larger effect on dengue reemergence compared to persistence. This can explain why, in Figure 2, there is more spatial variation observed in the average probabilities of dengue reemergence compared to persistence. Additionally, the strong positive association between population size and dengue reemergence means we would expect much longer periods of disease absence in the smaller districts compared to larger districts, which follows the well-known theories from Bartlett (1957). Interestingly, we

Table 2: Posterior means and 95% posterior credible intervals (in squared brackets) for the estimated parameters from the Markov chain part of the fitted ZS-CMSP model. Intercept row represents the average probabilities of reemergence and persistence with 0 neighbors infected i.e. $\text{expit}(\zeta_0)$ and $\text{expit}(\eta_0)$. Other rows represent the odds ratios i.e. $\exp(\zeta_k)$ and $\exp(\eta_k)$ for $k = \text{pop}=1, \dots, \text{Neighborhood Presence} = K + 1$. Neighborhood presence refers to the number of neighboring areas with the disease present during the previous month.

Covariate	Probability or Odds Ratio	
	Reemergence (absence to presence)	Persistence (presence to presence)
Intercept	.44 [.39-.50]	.88 [.86-.90]
pop (1000s)	1.024 [1.018-1.031]	1.009 [1.006-1.011]
HDI	1.173 [.277-5.044]	.791 [.254-2.471]
Temp _{t-1} (Celc.)	1.166 [1.121-1.214]	1.150 [1.115-1.187]
Rain _{t-1} (10 mm)	1.051 [1.030-1.074]	1.088 [1.070-1.107]
log(y _{i(t-1)} + 1)	–	5.697 [4.972-6.580]
Neighborhood Presence	1.226 [1.153-1.306]	1.074 [1.031-1.119]

found no association between human development index and the risk of dengue reemergence or persistence. Both rainfall and temperature have a strong positive association with dengue reemergence and persistence. For example, we estimated that a one degree rise in maximum temperature during the previous month is associated with a 16.6 [12.1-21.4] percent increase in the odds of dengue reemerging and a 15 [11.5-18.7] percent increase in the odds of dengue persisting. Therefore, we will have longer periods of disease absence during the winter (at least in the smaller districts) and longer periods of disease presence during the summer, which follows patterns in the mosquito population. The effects of both meteorological covariates on reemergence are not significantly different from their effects on persistence. It is interesting that the unique role played by the vertical transmission of dengue to mosquito eggs in the reemergence of dengue does not translate to different effects here, as rainfall and temperature both play a key role in the egg life cycle. The effect of the previous months cases, $\log y_{i(t-1)}$, on the persistence of the disease is quite large and reflects the fact that dengue will only go extinct when there is a small number of infected individuals.

The estimated spatial effects ("Neighborhood Presence" row of Table 2) show that the presence of dengue in neighboring districts is strongly associated with an increased risk of dengue reemergence and persistence. We estimated that dengue being present in a neighboring district during the previous month is associated with a 22.6 [15.3-30.6] percent increase

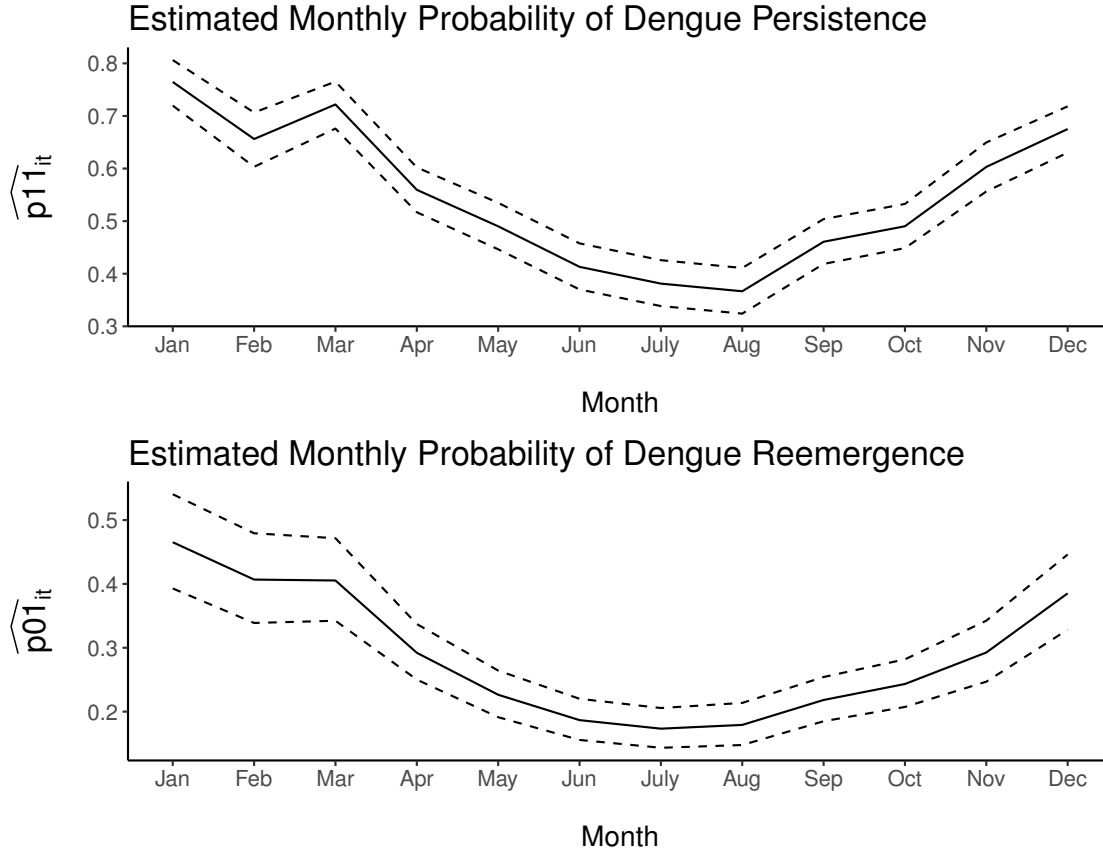


Figure 3: Posterior means (solid lines) and 95% posterior credible intervals (dashed lines) of the estimated monthly probabilities of dengue reemergence and persistence in a small district (pop=10,000). We assumed average monthly temperature and rainfall values, and 2 cases reported in the previous month for the persistence probabilities.

in the odds of dengue reemerging and 7.4 [3.1-11.9] percent increase in the odds of dengue persisting. The effect of neighboring dengue presence on reemergence is much higher than on persistence. Therefore, efforts to restrict cross infection between districts will be more effective if one district is not already infected. The width of the credible intervals for the odds ratios of the spatial parameters are relatively wide, which reflects the amount of hidden information involved in the estimation of these parameters (e.g. we do not always know if the disease is present in a neighboring district). Neighboring dengue presence may have a larger effect on the reemergence of dengue compared to the persistence due to a "spark" effect like with forest fires. For example, an individual infected by dengue will likely have a larger impact on the presence of the disease if they travel to an area without cases as opposed to an epidemic area, as the disease is likely to persist in the epidemic area anyway. This could also explain why population size also has a larger effect on the reemergence, since areas with high populations attract many visitors.

Table 3: Posterior means and 95% posterior credible intervals (in squared brackets) from the Poisson part of the fitted ZS-CMSP model.

Covariate	Parameter	Estimate
Intercept AR	β_0^{AR}	-.63 [-.65- -.61]
Rain _{t-1} (10 mm) AR	β_1	.17 [.16-.18]
Temp _{t-1} (C) AR	β_2	.284 [.281-.285]
Std. dev AR	σ_{AR}	.11 [.1-.13]
Intercept EN	β_0^{AR}	.92 [.81-1.02]
Std. dev EN	σ_{EN}	.63 [.55-.72]

Figure 3 shows posterior summaries of the estimated monthly probabilities of dengue reemergence and persistence for a small district (pop=10,000). To construct these, we assumed average monthly temperature and rainfall values, and 2 reported cases in the previous month for the persistence probabilities (as this is around the average number of cases reported before reported extinction in a small district). Note the figure shows $p01_{it} << p11_{it}$ at all times as expected. Figure 3 shows how the ZS-CMSP model can recreate the seasonal switching between periods of dengue presence and absence observed in the small districts. The estimated probability of dengue persistence drops to a low level during the winter leading to the likely extinction of the disease. The switch to the absent period lowers the estimated probability of disease presence further, as the estimated probability of dengue reemergence is much less than persistence. This can allow the disease to be absent for several months in a row. Then during the summer, the probability of disease reemergence rises leading to a good chance of disease presence. The switch to a period of presence means the disease will likely persist throughout the rest of the summer, as persistence has a much higher probability compared to reemergence (additionally the presence period will produce more cases in the summer leading to an increase in the probability of persistence until cases decline in the winter). The probability of disease reemergence never reaches above 50%, meaning it is reasonably possible for the disease to be absent for the entire year, which is observed in some districts.

Table 3 gives the estimated parameters from the Poisson part of the model. When dengue is present in a district, increases in temperature and rainfall lead to increased transmission of the disease. There is significant between district differences in the transmission rate and endemic risk. The differences in the endemic risk could be driven by either differences in the environment or reporting rates.

4.2 Fitted Values and Predictions

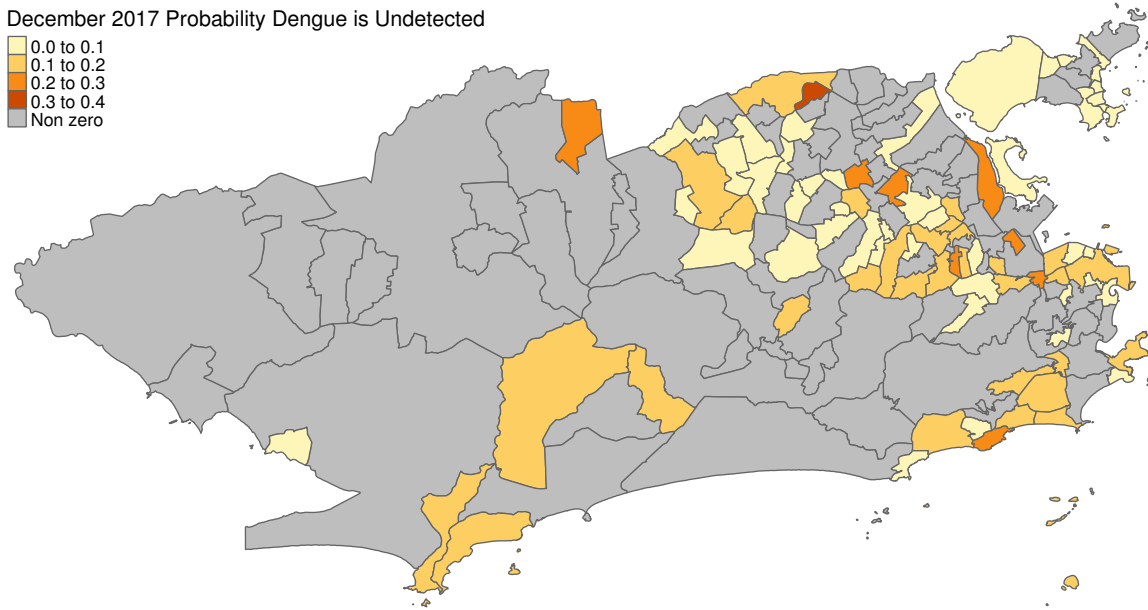


Figure 4: Posterior probability that dengue is undetected in districts reporting 0 cases for December 2017.

The underreporting of dengue cases is a major issue in Rio and the disease may frequently go undetected in some districts (Fernandes et al., 2009). Figure 4 shows a map of the posterior probability that dengue is undetected in districts reporting 0 cases for December 2017, the last month of the study period. The map shows the posterior mean of $S_{i,84}$ where ever $y_{i,84} = 0$, as explained in Section 3.2. The average probability that dengue is undetected in a district reporting 0 cases for this month is low, 11 percent. The posterior probability that dengue is undetected is highest in Parque Colúmbia, at 40 percent, where our model often estimates a high probability the disease is undetected. This district has never reported any cases which the model largely attributes to the disease often being undetected there (i.e. zeros are coming from the Poisson process), since the population size is similar to other districts that report cases and there are often cases reported in neighboring districts.

Figure 5 shows posterior summaries of the coupled one month ahead fitted values, see (16)-(17), of dengue cases (top graphs) and dengue presence (bottom graphs), for 4 districts. These were constructed by running the blocked forward filter in blocks with 2 neighboring locations, with each MCMC draw, as explained in Section 3.2. Generally, the model is able to predict, in sample, the presence of the disease one month ahead well when the disease is observed to be present. It is difficult to assess the presence fits when the disease is reportedly absent, as dengue could be undetected and actually present. A strong Markov dependence

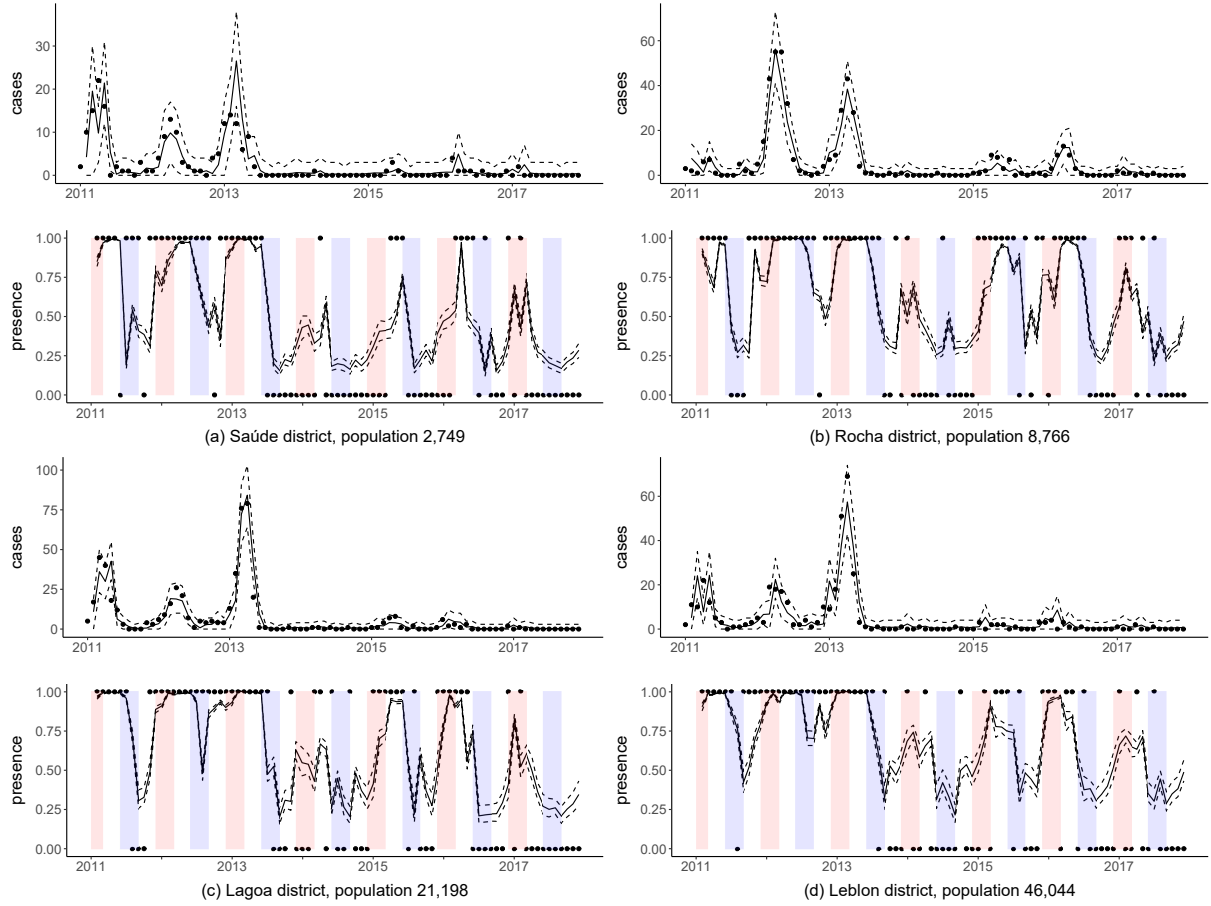


Figure 5: Posterior summaries of the coupled one month ahead fitted values for 4 districts. (top graphs) Coupled one month ahead fitted values of cases versus observed cases. (bottom graphs) Coupled one month ahead fitted values of dengue presence risk versus observed presence (0=0 reported cases which may not correspond to the actual absence of the disease). Posterior means (solid lines), 95% posterior credible intervals (dashed lines) and observed (points). Summer/winter seasons highlighted in red/blue in the bottom graphs.

can be seen in the presence fits, as when the disease has a high chance of being present it is usually predicted to be present again and when the disease has a high chance of being absent it is usually predicted to be absent again. Seasonal changes can modulate this pattern, however, with both fitted values rising during the summer and declining during the winter. The one month ahead fits of the cases seem to adequately capture the changing transmission intensity of the disease, with the cases generally rising and falling as expected by the model. However, the peak in the cases does not always follow what is predicted by the model, like during the 2011 and 2013 epidemics in the Saúde district. The one month ahead fits of the cases consistently capture consecutive zeros in the credible intervals.

Figure 6 shows summaries of the 1-12 month ahead posterior predictive distributions of dengue cases (top graphs) and dengue presence risk (bottom graphs) in two districts.

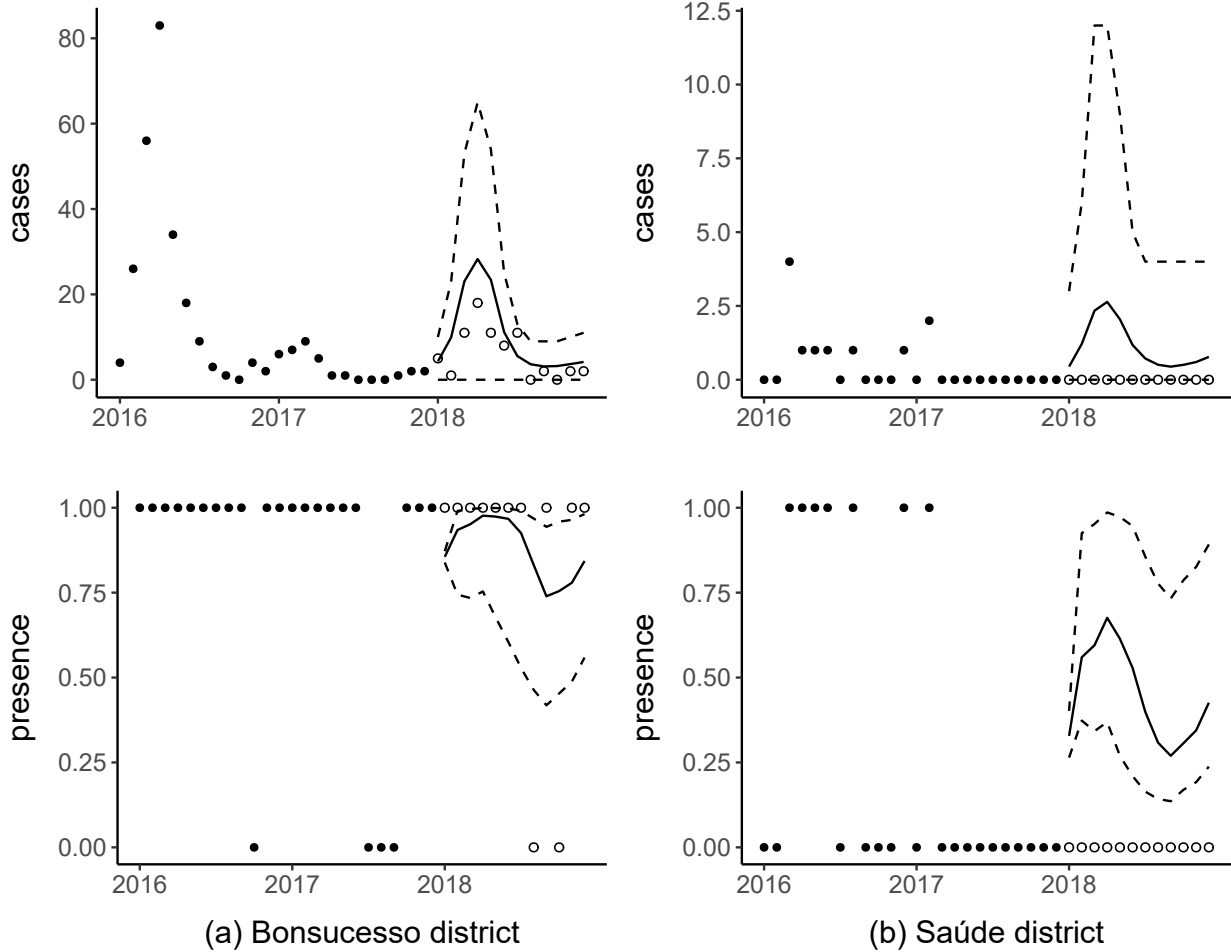


Figure 6: Summaries of the 1-12 month ahead posterior predictive distributions of the cases (top graphs) and dengue presence risk (bottom graphs) for 2 districts. Posterior predictive means (solid lines) and 95% posterior predictive credible intervals (dashed lines). Solid circles are from the last 2 years (2016-2017) used to fit the model and open circles are future observed values.

These were calculated using Algorithm 1 with $K = 12$. We assumed average monthly temperature and rainfall values in the calculations, although other forecasting scenarios could be considered, such as high temperature scenarios, or forecasts of the meteorological variables could be used. Both predictions of dengue presence and the case counts show a clear seasonal pattern, peaking in the summer and declining during the winter. The uncertainty in the predictions of dengue presence is large in both districts, meaning many future scenarios are possible. The top graphs, which show posterior predictive means and 95% posterior predictive credible intervals, can be misleading in this case as the posterior predictive distribution is zero inflated and, therefore, the density may not be concentrated around the mean (this is true for the top graphs in Figure 5 as well). SM Figures 4 and 5

show histograms of the 1-12 month ahead posterior predictive distributions of the cases in the same two districts, Saúde district in SM Figure 4 and Bonsucesso district in SM Figure 5. From SM Figure 4, there is always a very high posterior predictive probability of having 0 cases in a month, which may not be apparent from Figure 6 (b). SM Figure 5 illustrates how the zero inflation varies seasonally, with high amounts of zero inflation in the winter that declines in the summer. The predictions are clearly considering the possibility of seasonal switching between a period of presence in the summer and absence in the winter.

5 Concluding Remarks

We have proposed a zero-state coupled Markov switching Poisson (ZS-CMSP) model for general spatio-temporal infectious disease counts that contain an excess of zeros. The main difference with existing ZIP models used in spatio-temporal disease mapping is that the disease switches between periods of presence and absence in each area through a series of nonhomogeneous Markov chains coupled between neighboring locations, as opposed to the presence of the disease forming a series of conditionally independent Bernoulli random variables, which is presently the most popular approach. The difference is essentially between a finite mixture and finite Markov mixture model (Frühwirth-Schnatter, 2006), although we also introduce some spatial dependence in the states by coupling the partially hidden Markov chains between neighboring areas.

Our proposed model has several advantages over existing ZIP models used in epidemiology, which are largely nested in our model. Firstly, we model the reemergence of the disease separately from the persistence, and we can investigate whether a risk factor might affect the two events differently. This is justified as many important epidemiological risk factors can interact with the reemergence and persistence of an infectious disease in different ways, like temperature in the case of dengue (Coutinho et al., 2006). Secondly, as we model the probability of having a consecutive zero state separately from the probability of having a consecutive count state, we can consider long periods of disease absence in conjunction with long periods of disease presence, which are often observed in small areas. In contrast, the usual ZIP model can only consider long periods of disease absence or long periods of disease presence (not both). Thirdly, we consider spatio-temporal correlations in the presence of the disease without using random effects in the Bernoulli process, which often creates issues in interpretation and inference (Corpas-Burgos et al., 2018). Differently, in our proposed model, the correlations in disease presence are considered through a series of coupled Markov chains where the probabilities of disease reemergence and persistence can directly depend on the, potentially undetected, presence of the disease in neighboring areas. This

allows for straightforward interpretations about the correlations and provides temporal predictions that consider that the disease may be undetected in the area and neighboring areas. For the dengue example, the ZS-CMSP model fit better than the more traditional ZIP model and was able to reproduce the observed seasonal switching between long periods of disease presence and absence observed in the smaller districts.

Although we have applied the ZS-CMSP model to spatio-temporal infectious disease counts, it could be applied to data in other fields as well. For example, Malyshkina and Manner (2010) considered a zero state Markov switching count model, without coupling, for modeling traffic accidents across 335 highway segments in Indiana between 1995-1999. In their application, the zero state represented a low risk of accidents and the count state represented a high risk of accidents. It could be that a highway segment in the high risk state signals that nearby highway segments are also unsafe, and by coupling the chains between neighboring highways we could borrow strength between them to help determine the states.

There are also some limitations with our approach. Although the one month ahead fits are fairly accurate in most small districts there is some overdispersion in larger districts that the model has trouble capturing (not shown). A zero-state coupled Markov switching negative binomial model should be investigated in later works to help remedy this. Also, we are only considering disease presence in neighboring areas and, especially in a city, people often move around far outside their neighboring areas. It could be better to use a weighted sum of disease presence across all areas in the city, instead of just neighboring areas, where the weights could consider the relationship between areas, say based on cellphone data.

Acknowledgements

This work is part of the PhD thesis of D. Douwes-Schultz under the supervision of A. M. Schmidt in the Graduate Program of Biostatistics at McGill University, Canada. Schmidt is grateful for financial support from the Natural Sciences and Engineering Research Council (NSERC) of Canada (Discovery Grant RGPIN-2017-04999).

References

Adams, B. and Boots, M. (2010) How important is vertical transmission in mosquitoes for the persistence of dengue? Insights from a mathematical model. *Epidemics*, **2**, 1–10.

Aktekin, T. and Musal, M. (2015) Analysis of income inequality measures on human immunodeficiency virus mortality: A spatiotemporal Bayesian perspective. *Journal of the Royal Statistical Society: Series A*, **178**, 383–403.

Arab, A. (2015) Spatial and spatio-temporal models for modeling epidemiological data with excess zeros. *International Journal of Environmental Research and Public Health*, **12**, 10536–10548.

Bartlett, M. S. (1957) Measles periodicity and community size. *Journal of the Royal Statistical Society: Series A*, **120**, 48–60.

Bauer, C. and Wakefield, J. (2018) Stratified space–time infectious disease modelling, with an application to hand, foot and mouth disease in China. *Journal of the Royal Statistical Society Series C*, **67**, 1379–1398.

Besag, J. (1974) Spatial interaction and the statistical analysis of lattice systems. *Journal of the Royal Statistical Society: Series B*, **36**, 192–225.

Chan, T.-C., Hu, T.-H. and Hwang, J.-S. (2015) Daily forecast of dengue fever incidents for urban villages in a city. *International Journal of Health Geographics*, **14**, 9.

Chen, C. W. S., Khamthong, K. and Lee, S. (2019) Markov switching integer-valued generalized auto-regressive conditional heteroscedastic models for dengue counts. *Journal of the Royal Statistical Society: Series C*, **68**, 963–983.

Chib, S. (1996) Calculating posterior distributions and modal estimates in Markov mixture models. *Journal of Econometrics*, **75**, 79–97.

Corpas-Burgos, F., García-Donato, G. and Martínez-Beneito, M. A. (2018) Some findings on zero-inflated and hurdle Poisson models for disease mapping. *Statistics in Medicine*, **37**, 3325–3337.

Coutinho, F. A. B., Burattinia, M. N., Lopeza, L. F. and Massada, E. (2006) Threshold conditions for a non-autonomous epidemic system describing the population dynamics of dengue. *Bulletin of Mathematical Biology*, **68**, 2263–2282.

Diebold, F., Lee, J.-H. and Weinbach, G. (1993) Regime switching with time-varying transition probabilities. *Nonstationary Time Series Analysis and Cointegration*.

Fernandes, M. V. M., Schmidt, A. M. and Migon, H. S. (2009) Modelling zero-inflated spatio-temporal processes. *Statistical Modelling: An International Journal*, **9**, 3–25.

Frühwirth-Schnatter, S. (2006) *Finite Mixture and Markov Switching Models*. Springer Series in Statistics. New York: Springer-Verlag.

Gelman, A., Hwang, J. and Vehtari, A. (2014) Understanding predictive information criteria for Bayesian models. *Statistics and Computing*, **24**, 997–1016.

Goldfeld, S. M. and Quandt, R. E. (1973) A Markov model for switching regressions. *Journal of Econometrics*, **1**, 3–15.

Hamilton, J. D. (1989) A new approach to the economic analysis of nonstationary time series and the business cycle. *Econometrica*, **57**, 357–384.

— (1993) 9 Estimation, inference and forecasting of time series subject to changes in regime. In *Handbook of Statistics*, vol. 11 of *Econometrics*, 231–260. Elsevier.

Lambert, D. (1992) Zero-inflated Poisson regression, with an application to defects in manufacturing. *Technometrics*, **34**, 1–14.

Malyshkina, N. V. and Mannerling, F. L. (2010) Zero-state Markov switching count-data models: An empirical assessment. *Accident Analysis & Prevention*, **42**, 122–130.

Marquardt, W. H. (ed.) (2004) *Biology of Disease Vectors*. Burlington, MA: Academic Press, 2nd edition edn.

Okano, J. T., Sharp, K., Valdano, E., Palk, L. and Blower, S. (2020) HIV transmission and source–sink dynamics in sub-Saharan Africa. *The Lancet HIV*, **7**, e209–e214.

Plummer, M., Best, N., Cowles, K. and Vines, K. (2006) CODA: Convergence diagnosis and output analysis for MCMC. *R News*, **6**, 7–11.

Pohle, J., Langrock, R., van der Schaar, M., King, R. and Jensen, F. H. (2020) A primer on coupled state-switching models for multiple interacting time series. *Statistical Modelling*.

Roberts, G. O. and Sahu, S. K. (1997) Updating schemes, correlation structure, blocking and parameterization for the Gibbs sampler. *Journal of the Royal Statistical Society: Series B*, **59**, 291–317.

Schmidt, W.-P., Suzuki, M., Thiem, V. D., White, R. G., Tsuzuki, A., Yoshida, L.-M., Yanai, H., Haque, U., Tho, L. H., Anh, D. D. and Ariyoshi, K. (2011) Population density, water supply, and the risk of dengue fever in Vietnam: Cohort study and spatial analysis. *PLOS Medicine*, **8**, e1001082.

Scott, S. L. (2002) Bayesian methods for hidden Markov models. *Journal of the American Statistical Association*, **97**, 337–351.

Shaby, B. A. and Wells, M. T. (2010) Exploring an adaptive Metropolis algorithm.

Spezia, L., Brewer, M. J. and Birkel, C. (2017) An anisotropic and inhomogeneous hidden Markov model for the classification of water quality spatio-temporal series on a national scale: The case of Scotland. *Environmetrics*, **28**, e2427.

Stoddard, S. T., Forshey, B. M., Morrison, A. C., Paz-Soldan, V. A., Vazquez-Prokopec, G. M., Astete, H., Reiner, R. C., Vilcarromero, S., Elder, J. P., Halsey, E. S., Kochel, T. J., Kitron, U. and Scott, T. W. (2013) House-to-house human movement drives dengue virus transmission. *Proceedings of the National Academy of Sciences of the United States of America*, **110**, 994–999.

Touloupou, P., Finkenstädt, B. and Spencer, S. E. F. (2020) Scalable Bayesian inference for coupled hidden Markov and semi-Markov models. *Journal of Computational and Graphical Statistics*, **29**, 238–249.

de Valpine, P., Turek, D., Paciorek, C. J., Anderson-Bergman, C., Lang, D. T. and Bodik, R. (2017) Programming with models: Writing statistical algorithms for general model structures with NIMBLE. *Journal of Computational and Graphical Statistics*, **26**, 403–413.

Vergne, T., Korennoy, F., Combelles, L., Gogin, A. and Pfeiffer, D. U. (2016) Modelling African swine fever presence and reported abundance in the Russian Federation using national surveillance data from 2007 to 2014. *Spatial and Spatio-temporal Epidemiology*, **19**, 70–77.

Wang, P. (2001) Markov zero-inflated Poisson regression models for a time series of counts with excess zeros. *Journal of Applied Statistics*, **28**, 623–632.

Wangdi, K., Clements, A. C. A., Du, T. and Nery, S. V. (2018) Spatial and temporal patterns of dengue infections in Timor-Leste, 2005–2013. *Parasites & Vectors*, **11**, 9.

Young, D. S., Roemmele, E. S. and Shi, X. (2020) Zero-inflated modeling part II: Zero-inflated models for complex data structures. *WIREs Computational Statistics*, e1540.

Supplementary material for “A zero-state coupled Markov switching Poisson model for spatio-temporal infectious disease counts”

Dirk Douwes-Schultz* and Alexandra M. Schmidt

Department of Epidemiology, Biostatistics and Occupational Health

McGill University, Canada

February 28, 2025

Contents

1	The blocked forward filtering backward sampling (bFFBS) algorithm	1
1.1	Validating the algorithm	4
2	Simulation study	5
3	Monte Carlo Approximations for the Posterior Predictive Distributions	8
4	Posterior Predictive Histograms	10
1	The blocked forward filtering backward sampling (bFFBS) algorithm	

Borrowing the notation from the main text, sampling \mathbf{S} in the Gibbs sampler involves the following. First we initialize $\mathbf{S}^{[1]}$ by setting $S_{it}^{[1]} = 0$ whenever $y_{it} = 0$, and we set $S_{it}^{[m]} = 1$ whenever $y_{it} > 0$ for all m , since only the Poisson process can produce a positive count. Then the following steps are repeated for $m = 1, \dots, Q$,

*Corresponding author: Dirk Douwes-Schultz, Department of Epidemiology, Biostatistics and Occupational Health, McGill University, 1020 Pine Avenue, Montreal, QC, Canada, H3A 1A2. E-mail: dirk.douwes-schultz@mail.mcgill.ca.

1. Sample $\mathbf{v}^{[m]}$ from $p(\mathbf{v} | \mathbf{S}^{[m-1]}, \mathbf{y})$
2. Sample $\mathbf{S}_{(c)}^{[m]}$ from $p(\mathbf{S}_{(c)} | \mathbf{S}_{(1)}^{[m]}, \dots, \mathbf{S}_{(c-1)}^{[m]}, \mathbf{S}_{(c+1)}^{[m-1]}, \dots, \mathbf{S}_{(C)}^{[m-1]}, \mathbf{v}^{[m]}, \mathbf{y})$ for $c = 1, \dots, C$.

Step 1 is broken up into (mostly) Metropolis-Hastings steps as described in the main text. In step 2, we only sample unknown (i.e. when $y_{it} = 0$) state indicators in the block. Here we provide the algorithms for sampling from $p(\mathbf{S}_{(c)} | \mathbf{S}_{(-c)}, \mathbf{v}, \mathbf{y})$ needed for step 2. Toulouppou et al. (2020) derived the algorithm for $n_c = 1$ for all c , and it is straightforward to generalize it to arbitrary n_c .

Note that,

$$\begin{aligned} p(\mathbf{S}_{(c)} | \mathbf{S}_{(-c)}, \mathbf{y}, \mathbf{v}) &= p(\mathbf{S}_{(c)T} | \mathbf{S}_{(-c)(0:T)}, \mathbf{y}, \mathbf{v}) \\ &\times \prod_{t=0}^{T-1} p(\mathbf{S}_{(c)t} | \mathbf{S}_{(c)t+1}, \mathbf{S}_{(-c)(0:t+1)}, \mathbf{y}_{(1:N)(1:t)}, \mathbf{v}). \end{aligned} \quad (1)$$

and that,

$$\begin{aligned} p(\mathbf{S}_{(c)t} | \mathbf{S}_{(c)t+1}, \mathbf{S}_{(-c)(0:t+1)}, \mathbf{y}_{(1:N)(1:t)}, \mathbf{v}) &\propto p(\mathbf{S}_{(c)(t+1)} | \mathbf{S}_{(c)(t)}, \mathbf{S}_{(-c)(t)}, \mathbf{y}_{(1:N)(1:t)}, \mathbf{v}) \\ &\times p(\mathbf{S}_{(c)t} | \mathbf{S}_{(-c)(0:t+1)}, \mathbf{y}_{(1:N)(1:t)}, \mathbf{v}). \end{aligned}$$

Now, $P(\mathbf{S}_{(c)t} = \mathbf{s}_{(c)t} | \mathbf{S}_{(-c)(0:t+1)}, \mathbf{y}_{(1:N)(1:t)}, \mathbf{v})$ for $t = 0, \dots, T$ and $\mathbf{s}_{(c)t} \in \{0, 1\}^{n_c}$ are known as the filtered probabilities. These are calculated using the forward part of the bFFBS algorithm, starting with $t = 0$, we have,

$$P(\mathbf{S}_{(c)0} = \mathbf{s}_{(c)0} | \mathbf{S}_{(-c)(0:1)}, \mathbf{v}) \propto \prod_{j \in (-c)} p(S_{j1} | \mathbf{S}_{(c)0} = \mathbf{s}_{(c)0}, \mathbf{S}_{(-c)0}, \mathbf{v}) \prod_{i \in c} P(S_{i0} = s_{i0}(\mathbf{s}_{(c)0})),$$

where $s_{i0}(\mathbf{s}_{(c)0})$ is the state indicator for location i in $\mathbf{s}_{(c)0}$. Now for $t = 1, \dots, T$ the predictive probabilities are first calculated and then used to calculate the filtered probabilities. The predictive probability is given by,

$$\begin{aligned} P(\mathbf{S}_{(c)t} = \mathbf{s}_{(c)t} | \mathbf{S}_{(-c)(0:t)}, \mathbf{y}_{(1:N)(1:t-1)}, \mathbf{v}) &= \\ \sum_{\mathbf{s}'_{(c)t-1} \in \{0, 1\}^{n_c}} P(\mathbf{S}_{(c)t} = \mathbf{s}_{(c)t} | \mathbf{S}_{(c)(t-1)} = \mathbf{s}'_{(c)t-1}, \mathbf{S}_{(-c)(t-1)}, \mathbf{y}_{(1:N)(1:t-1)}, \mathbf{v}) &\quad (2) \\ \times P(\mathbf{S}_{(c)(t-1)} = \mathbf{s}'_{(c)t-1} | \mathbf{S}_{(-c)(0:t)}, \mathbf{y}_{(1:N)(1:t-1)}, \mathbf{v}), \end{aligned}$$

which is most efficiently calculated by multiplying the $2^{n_c} \times 2^{n_c}$ conditional transition matrix of $\mathbf{S}_{(c)t}$, $\Gamma(\mathbf{S}_{(c)t} | \mathbf{S}_{(-c)(t-1)}, \mathbf{y}_{(1:N)(1:t-1)})$, transposed by the vector of previous filtered

probabilities. Note that an element of $\Gamma(\mathbf{S}_{(c)t} | \mathbf{S}_{(-c)(t-1)}, \mathbf{y}_{(1:N)(1:t-1)})$ is given by,

$$P(\mathbf{S}_{(c)t} = \mathbf{s}_{(c)t} | \mathbf{S}_{(c)(t-1)} = \mathbf{s}'_{(c)t-1}, \mathbf{S}_{(-c)(t-1)}, \mathbf{y}_{(1:N)(1:t-1)}, \mathbf{v}) = \prod_{i \in c} P(S_{it} = s_{it}(\mathbf{s}_{(c)t}) | \mathbf{S}_{(c)(t-1)} = \mathbf{s}'_{(c)t-1}, \mathbf{S}_{(-c)(t-1)}, \mathbf{y}_{(1:N)(1:t-1)}, \mathbf{v}),$$

where $s_{it}(\mathbf{s}_{(c)t})$ is the state indicator for location i in $\mathbf{s}_{(c)t}$, which can be calculated from the individual area conditional transition matrices defined in equation (1) of the main text. The predictive probabilities are then used to calculate the filtered probabilities,

$$\begin{aligned} P(\mathbf{S}_{(c)t} = \mathbf{s}_{(c)t} | \mathbf{S}_{(-c)(0:t+1)}, \mathbf{y}_{(1:N)(1:t)}, \mathbf{v}) &\propto \\ P(\mathbf{S}_{(c)t} = \mathbf{s}_{(c)t} | \mathbf{S}_{(-c)(0:t)}, \mathbf{y}_{(1:N)(1:t-1)}, \mathbf{v}) \prod_{i \in c} p(y_{it} | S_{it} = s_{it}(\mathbf{s}_{(c)t}), \mathbf{y}_{(1:N)(1:t-1)}, \mathbf{v}) \\ \times \prod_{j \in (-c)} p(S_{j(t+1)} | \mathbf{S}_{(c)t} = \mathbf{s}_{(c)t}, \mathbf{S}_{(-c)t}, \mathbf{y}_{(1:N)(1:t)}, \mathbf{v}), \end{aligned} \quad (3)$$

which involves the predictive probability. In (3), if $y_{it} > 0$ and $s_{it}(\mathbf{s}_{(c)t}) = 0$, then $p(y_{it} | S_{it} = s_{it}(\mathbf{s}_{(c)t}), \mathbf{y}_{(1:N)(1:t-1)}, \mathbf{v}) = 0$. This means the entire filtered probability can be set to 0 and, therefore, these conditions should be checked first to avoid unnecessary calculations. In the extreme case where $y_{it} > 0$ for all $i \in c$, then t can be skipped altogether as the entire vector of filtered probabilities is then known. Also, if $y_{it} > 0$ but $s_{it}(\mathbf{s}_{(c)t}) = 1$ then $p(y_{it} | S_{it} = s_{it}(\mathbf{s}_{(c)t}), \mathbf{y}_{(1:N)(1:t-1)}, \mathbf{v})$ can be set to 1, since it will cancel in the calculation when normalizing. For $t = T$, there is no $\prod_{j \in (-c)} p(S_{j(t+1)} | \mathbf{S}_{(c)t} = \mathbf{s}_{(c)t}, \mathbf{S}_{(-c)t}, \mathbf{y}_{(1:N)(1:t)}, \mathbf{v})$ term included.

After all filtered probabilities have been calculated then the backward sampling step is performed. Starting at $T = t$, $\mathbf{S}_{(c)T}^{[m]}$ is sampled categorically from the final filtered probabilities. Then, for $t = T-1, \dots, 0$ we sample $\mathbf{S}_{(c)t}^{[m]}$ from,

$$\begin{aligned} P(\mathbf{S}_{(c)t}^{[m]} = \mathbf{s}_{(c)t} | \mathbf{S}_{(c)(t+1)}^{[m]}, \mathbf{S}_{(-c)(0:t+1)}, \mathbf{y}_{(1:N)(1:t)}, \mathbf{v}) &\propto \\ p(\mathbf{S}_{(c)(t+1)}^{[m]} | \mathbf{S}_{(c)t}^{[m]} = \mathbf{s}_{(c)t}, \mathbf{S}_{(-c)t}, \mathbf{y}_{(1:N)(1:t)}, \mathbf{v}) \\ \times P(\mathbf{S}_{(c)t}^{[m]} = \mathbf{s}_{(c)t} | \mathbf{S}_{(-c)(0:t+1)}, \mathbf{y}_{(1:N)(1:t)}, \mathbf{v}). \end{aligned} \quad (4)$$

The first probability in (4) comes from $\Gamma(\mathbf{S}_{(c)(t+1)} | \mathbf{S}_{(-c)t}, \mathbf{y}_{(1:N)(1:t)})$, the second probability is the filtered probability. Note that when $y_{it} > 0$ the algorithm will always sample $S_{it}^{[m]} = 1$ and, therefore, these can just be set ahead of running the MCMC as mentioned.

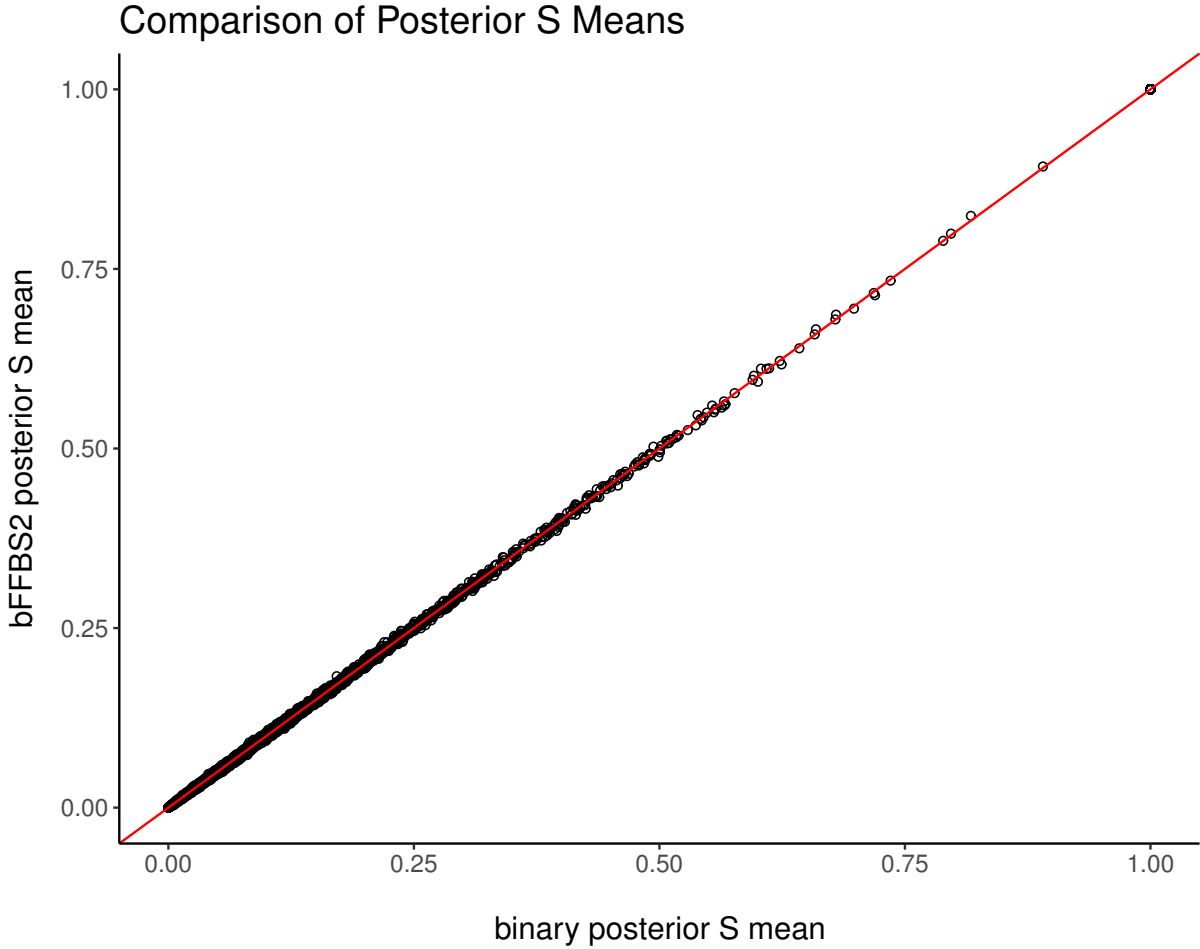


Figure 1: Comparison of the posterior means of \mathbf{S} produced by the binary and bFFBS2 samplers.

1.1 Validating the algorithm

To validate the bFFBS algorithm, we compared the posteriors produced by the bFFBS2 sampler, described in the main text, with those produced by the binary sampler. These were compared on the dengue data, whose fitting is described in the main text. The binary sampler is validated in the simulation study in Section 2 of this appendix. Therefore, the bFFBS2 sampler should produce the same posterior distributions as the binary sampler.

In Figure 1, we show a plot comparing the posterior means of \mathbf{S} from the two samplers. Both samplers produce the same posterior means for \mathbf{S} within reasonable Monte Carlo error. Additionally, we compared the posterior means and 95% posterior credible intervals for all elements of \mathbf{v} (not shown). There was no meaningful difference in the posteriors of \mathbf{v} produced by the two samplers.

2 Simulation study

We designed a simulation study to ensure the proposed hybrid Gibbs sampler can recover the true parameters of the ZS-CMSP model. In addition, our simulation study investigates the consequences of model misspecification and not accounting for the imperfect detection of the disease. The specification of λ_{it} will affect the estimation of $\boldsymbol{\theta}$ and \mathbf{S} . Therefore, proper specification of λ_{it} could be important for obtaining valid inferences about the reemergence and persistence of the disease being studied. We generated data from a ZS-CMSP model with the following specification for λ_{it} and \mathbf{z}_{it} ,

$$\begin{aligned}\log(\lambda_{it}) &= \beta_0 + \beta_1 \text{Temp}_{t-1} + \beta_2 \text{HDI}_i, \\ \mathbf{z}_{it} &= [\text{Temp}_{t-1}]^T,\end{aligned}\tag{5}$$

where $\mathbf{v} = [\beta_0, \beta_1, \beta_2, \zeta_0, \zeta_1, \zeta_2, \eta_0, \eta_1, \eta_2]^T = [1, .1, 10, -1.5, .1, .1, 1.5, .05, .25]^T$ and the covariates are taken from the motivating example in the main text, for $i = 1, \dots, 160$ and $t = 1, \dots, 84$ like the motivating example. Additionally we assumed $p(S_{i0}) \sim \text{Bern}(.5)$ for $i = 1, \dots, N$. We fit three models using the proposed hybrid Gibbs sampler to the data generated by (5): a correctly specified ZS-CMSP model (M1); an incorrectly specified ZS-CMSP model that does not include HDI as a covariate for λ_{it} (M2) and, finally, a model that assumes perfect detection of disease presence based on the reported case counts (M3). The M3 model erroneously assumed that $S_{it} = 1$ when $y_{it} > 0$ and that $S_{it} = 0$ when $y_{it} = 0$. In this case \mathbf{S} is fully observed and we only sampled $\boldsymbol{\theta}$ in the Gibbs sampler. Otherwise, for M1 and M2, \mathbf{S} was sampled using one at a time sampling since convergence of the MCMC algorithm was fast. We ran 20,000 iterations, with a burn-in of 10,000, of the Gibbs sampler on 3 chains started randomly from different points. For each replication, convergence of each parameter was checked using the effective sample size (>1000) and the Gelman-Rubin statistic (<1.05) (Plummer et al., 2006). No parameter during any replication failed to converge.

The sampling distribution of the posterior means for each fitted model from 100 replications can be seen in Figure 2. The hybrid Gibbs sampler can recover the parameters of the properly specified ZS-CMSP model with minimal bias. However, the estimates from the misspecified ZS-CMSP model (M2) and the model assuming perfect detection (M3) are badly biased for some parameters. For example, M3 underestimates the effect of temperature on reemergence (ζ_1) by a factor of one half on average. This simulation study shows that it is important to account for imperfect detection with a zero inflated model and to correctly specify λ_{it} . We recommend using coupled one step ahead fitted values to diagnose model misspecification (see Section 3.2 of the main text).

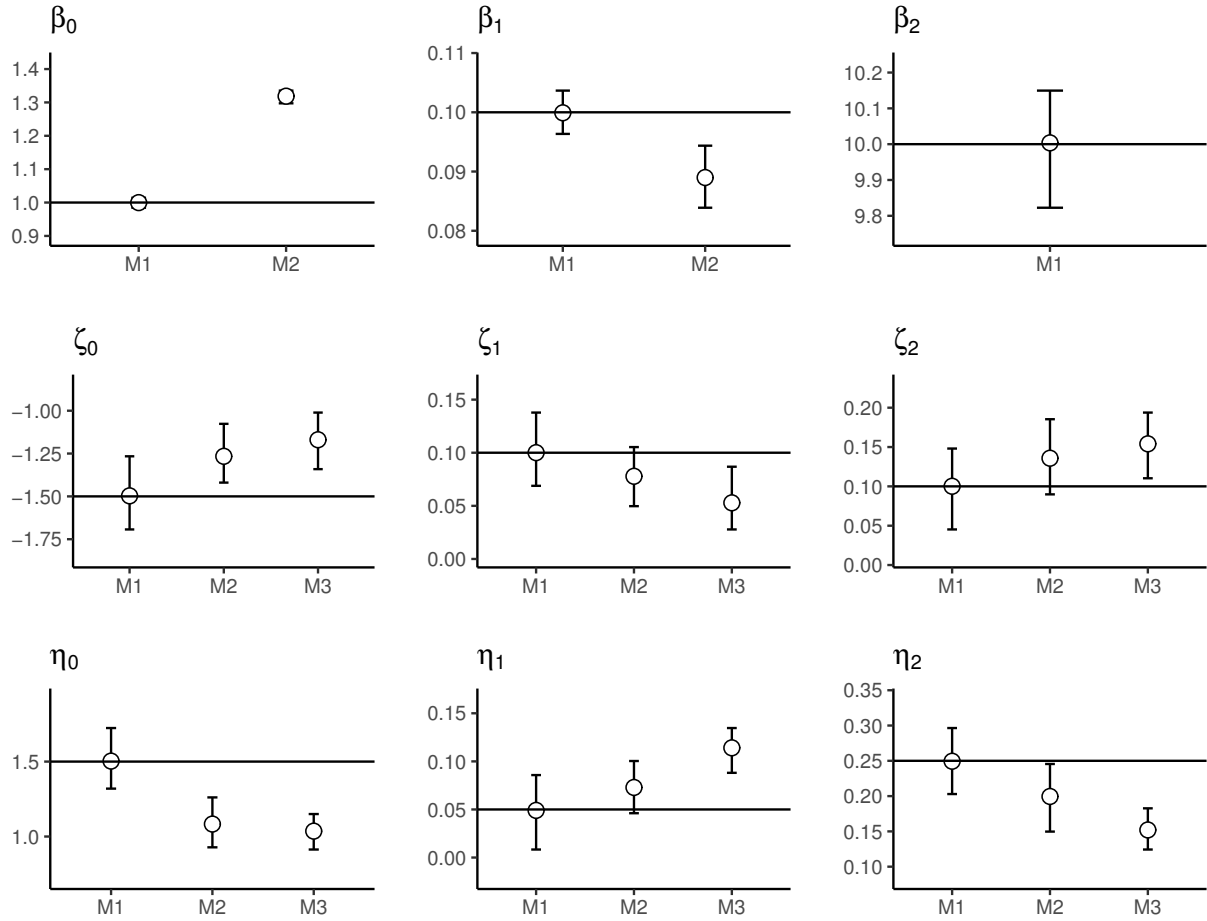


Figure 2: Average and 95% quantile for the sampling distribution, from 100 simulations, of the posterior means estimated with the proposed Gibbs sampler. M1 - correctly specified ZS-CMSP, M2 - misspecified ZS-CMSP and M3 - assuming perfect detection. Horizontal lines drawn at true parameter values.

Finally, as the popular ZIP model is nested within the ZS-CMSP model, we wanted to ensure that the ZS-CMSP model could return the true parameters if the ZIP model generates the data. Therefore, we ran another set of 100 replications of (5) with $\boldsymbol{v} = [\beta_0, \beta_1, \beta_2, \zeta_0, \zeta_1, \zeta_2, \eta_0, \eta_1, \eta_2]^T = [1, .1, 10, .5, .1, 0, .5, .1, 0]^T$ which corresponds to a ZIP model. We then fit the replicates with the hybrid Gibbs sampler for the ZS-CMSP model. The sampling distribution of the posterior mean from 100 replications can be seen in Figure 3. The hybrid Gibbs sampler for the ZS-CMSP model can recover the correct parameter values when the corresponding ZIP model generates the data. This means the ZS-CMSP model can be fit to general spatio-temporal data sets with excess zeros and it should be clear from the parameter estimates if the simpler ZIP model is more appropriate.

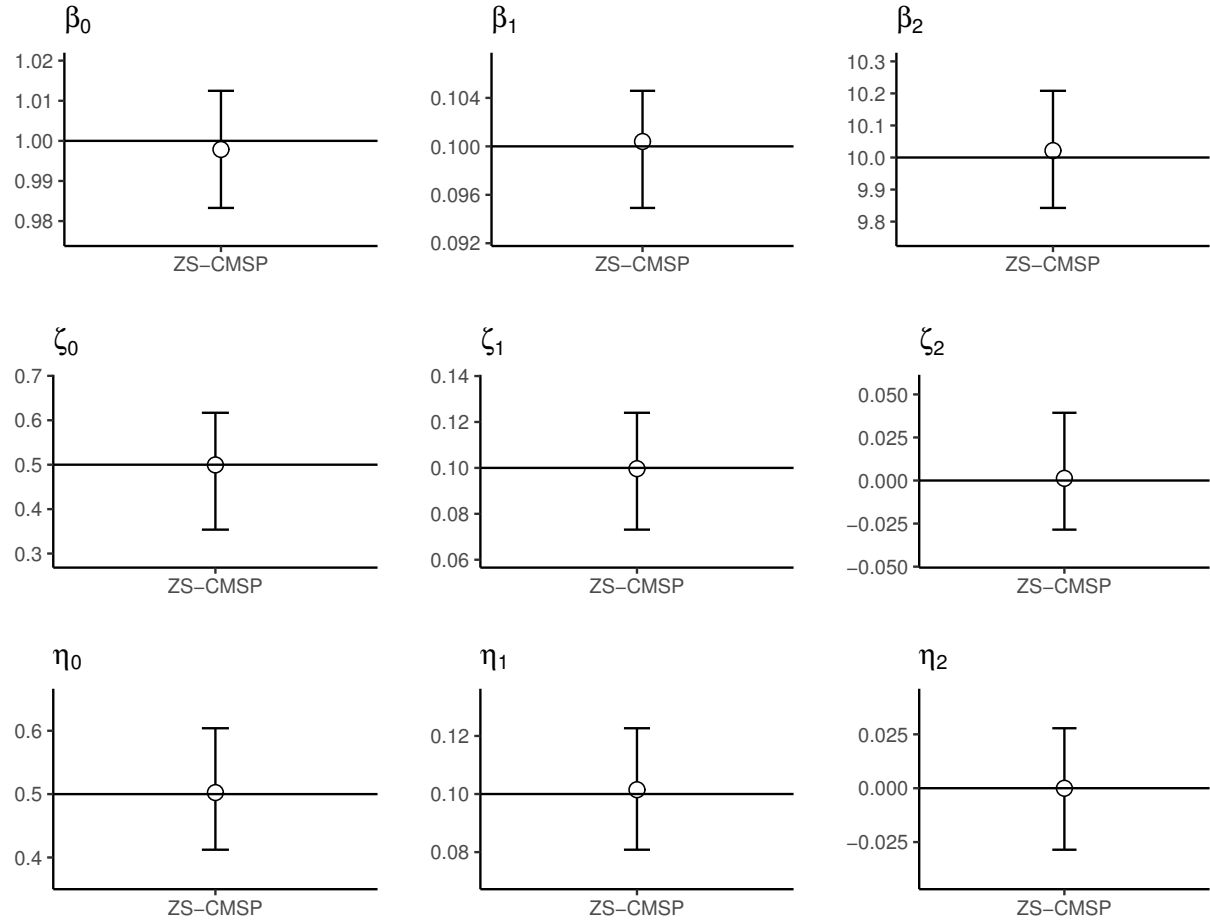


Figure 3: Average and 95% quantile for the sampling distribution, from 100 simulations, of the posterior means estimated with the proposed Gibbs sampler. Horizontal lines drawn at true parameter values which corresponds to a ZIP model.

3 Monte Carlo Approximations for the Posterior Predictive Distributions

We are interested in the K step ahead posterior predictive distribution of both disease presence, $p(S_{i(T+K)}|\mathbf{y})$, and the cases counts, $p(y_{i(T+K)}|\mathbf{y})$, for $K = 1, 2, \dots$ and $i = 1, \dots, N$. We assume only dependence on the previous times counts for simplicity in notation, then we have,

$$\begin{aligned} p(S_{i(T+K)}|\mathbf{y}) &= \int p(S_{i(T+K)}|\mathbf{S}_{T+K-1}, \mathbf{y}_{T+K-1}, \boldsymbol{\theta}) \\ &\quad \times p(\mathbf{y}_{T+K-1}|\mathbf{S}_{T+K-1}, \mathbf{y}_{T+K-2}, \boldsymbol{\beta}) p(\mathbf{S}_{T+K-1}|\mathbf{S}_{T+K-2}, \mathbf{y}_{T+K-2}, \boldsymbol{\theta}) \quad (6) \\ &\quad \dots \times p(\mathbf{y}_{T+1}|\mathbf{S}_{T+1}, \mathbf{y}_T, \boldsymbol{\beta}) p(\mathbf{S}_{T+1}|\mathbf{S}_T, \mathbf{y}_T, \boldsymbol{\theta}) \\ &\quad \times p(\mathbf{v}|\mathbf{y}) d\mathbf{y}_{T+K-1} d\mathbf{S}_{T+K-1} \dots d\mathbf{y}_{T+1} d\mathbf{S}_{T+1} d\boldsymbol{\beta} d\boldsymbol{\theta}, \end{aligned}$$

and,

$$\begin{aligned} p(y_{i(T+K)}|\mathbf{y}) &= \int p(y_{i(T+K)}|S_{i(T+K)}, \mathbf{y}_{T+K-1}, \boldsymbol{\beta}) p(S_{i(T+K)}|\mathbf{S}_{T+K-1}, \mathbf{y}_{T+K-1}, \boldsymbol{\theta}) \\ &\quad \times p(\mathbf{y}_{T+K-1}|\mathbf{S}_{T+K-1}, \mathbf{y}_{T+K-2}, \boldsymbol{\beta}) p(\mathbf{S}_{T+K-1}|\mathbf{S}_{T+K-2}, \mathbf{y}_{T+K-2}, \boldsymbol{\theta}) \\ &\quad \dots \times p(\mathbf{y}_{T+1}|\mathbf{S}_{T+1}, \mathbf{y}_T, \boldsymbol{\beta}) p(\mathbf{S}_{T+1}|\mathbf{S}_T, \mathbf{y}_T, \boldsymbol{\theta}) \\ &\quad \times p(\mathbf{v}|\mathbf{y}) dS_{i(T+K)} d\mathbf{y}_{T+K-1} d\mathbf{S}_{T+K-1} \dots d\mathbf{y}_{T+1} d\mathbf{S}_{T+1} d\boldsymbol{\beta} d\boldsymbol{\theta} \\ &= \int [p(y_{i(T+K)}|S_{i(T+K)} = 1, \mathbf{y}_{T+K-1}, \boldsymbol{\beta}) P(S_{i(T+K)} = 1|\mathbf{S}_{T+K-1}, \mathbf{y}_{T+K-1}, \boldsymbol{\theta}) \\ &\quad + I[y_{i(T+K)} = 0] (1 - P(S_{i(T+K)} = 1|\mathbf{S}_{T+K-1}, \mathbf{y}_{T+K-1}, \boldsymbol{\theta}))] \\ &\quad \times p(\mathbf{y}_{T+K-1}|\mathbf{S}_{T+K-1}, \mathbf{y}_{T+K-2}, \boldsymbol{\beta}) p(\mathbf{S}_{T+K-1}|\mathbf{S}_{T+K-2}, \mathbf{y}_{T+K-2}, \boldsymbol{\theta}) \\ &\quad \dots \times p(\mathbf{y}_{T+1}|\mathbf{S}_{T+1}, \mathbf{y}_T, \boldsymbol{\beta}) p(\mathbf{S}_{T+1}|\mathbf{S}_T, \mathbf{y}_T, \boldsymbol{\theta}) \\ &\quad \times p(\mathbf{v}|\mathbf{y}) d\mathbf{y}_{T+K-1} d\mathbf{S}_{T+K-1} \dots d\mathbf{y}_{T+1} d\mathbf{S}_{T+1} d\boldsymbol{\beta} d\boldsymbol{\theta}. \quad (7) \end{aligned}$$

The above integrals can be approximated through Monte Carlo integration,

$$p(S_{i(T+K)}|\mathbf{y}) \approx \frac{1}{Q-M} \sum_{m=M+1}^Q p(S_{i(T+K)}^{[m]}|\mathbf{S}_{T+K-1}^{[m]}, \mathbf{y}_{T+K-1}^{[m]}, \boldsymbol{\theta}^{[m]}), \quad (8)$$

and,

$$\begin{aligned}
p(y_{i(T+K)} | \mathbf{y}) \approx & \frac{1}{Q-M} \sum_{m=M+1}^Q \left[p(y_{i(T+K)} | S_{i(T+K)} = 1, \mathbf{y}_{T+K-1}^{[m]}, \boldsymbol{\beta}^{[m]}) P(S_{i(T+K)} = 1 | \mathbf{S}_{T+K-1}^{[m]}, \mathbf{y}_{T+K-1}^{[m]}, \boldsymbol{\theta}^{[m]}) \right. \\
& \left. + I[y_{i(T+K)} = 0] \left(1 - P(S_{i(T+K)} = 1 | \mathbf{S}_{T+K-1}^{[m]}, \mathbf{y}_{T+K-1}^{[m]}, \boldsymbol{\theta}^{[m]}) \right) \right], \tag{9}
\end{aligned}$$

where the superscript $[m]$ denotes a draw from the posterior distribution of the variable ($\mathbf{y}_t^{[m]} = \mathbf{y}_t$ if $t \leq T$), M is the size of the burn-in sample, Q is the total MCMC sample size and $I[\cdot]$ is an indicator function. Substituting $K = 1$ into (8)-(9) gives equations (11)-(12) in the main text.

4 Posterior Predictive Histograms

Figures 4 and 5 show histograms of the 1-12 month ahead posterior predictive distributions of the cases in the same two districts shown in Figure 6 of the main text, Saúde district in Figure 4 and Bonsucesso district in Figure 5.

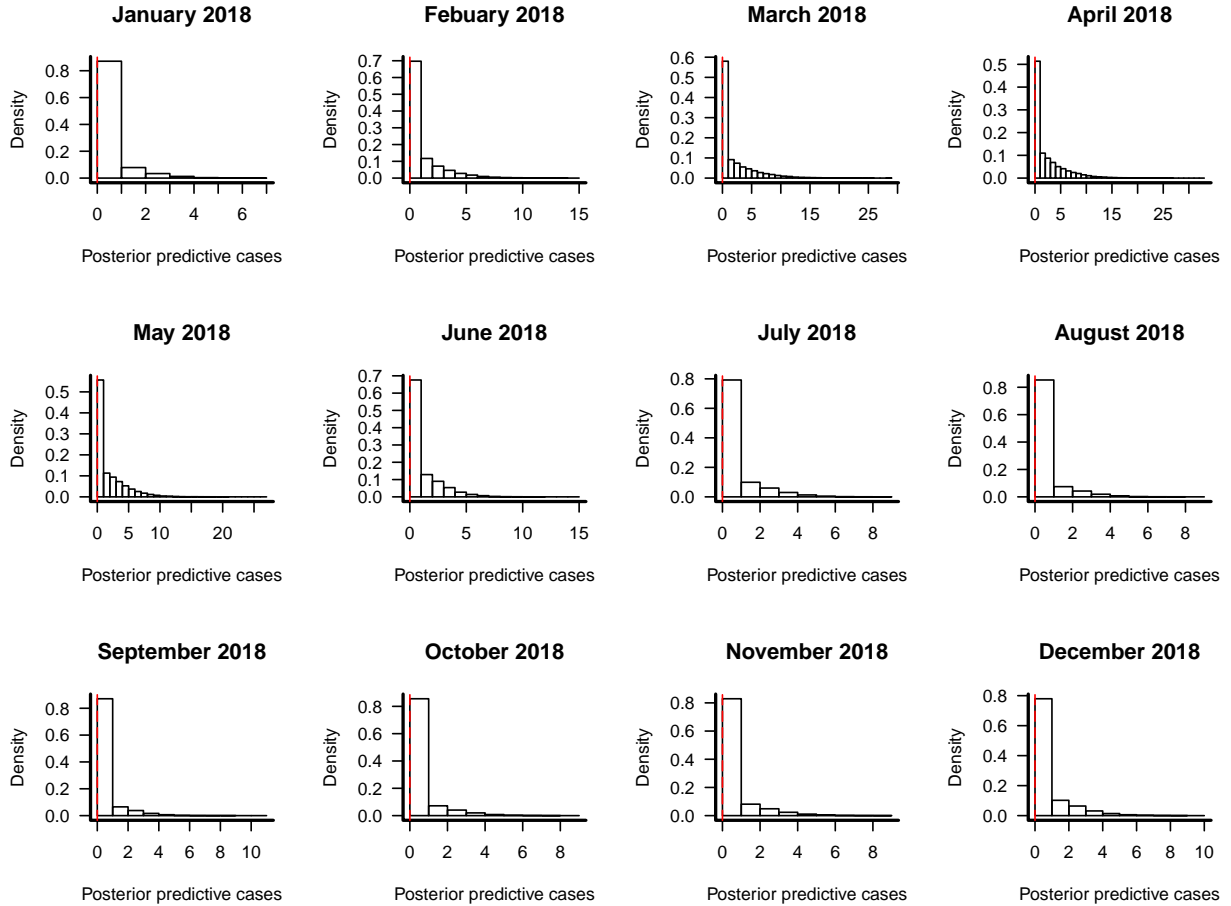


Figure 4: Histograms of the 1-12 month ahead posterior predictive distributions of the cases in the Saúde district. Red dotted line represents the observed values.

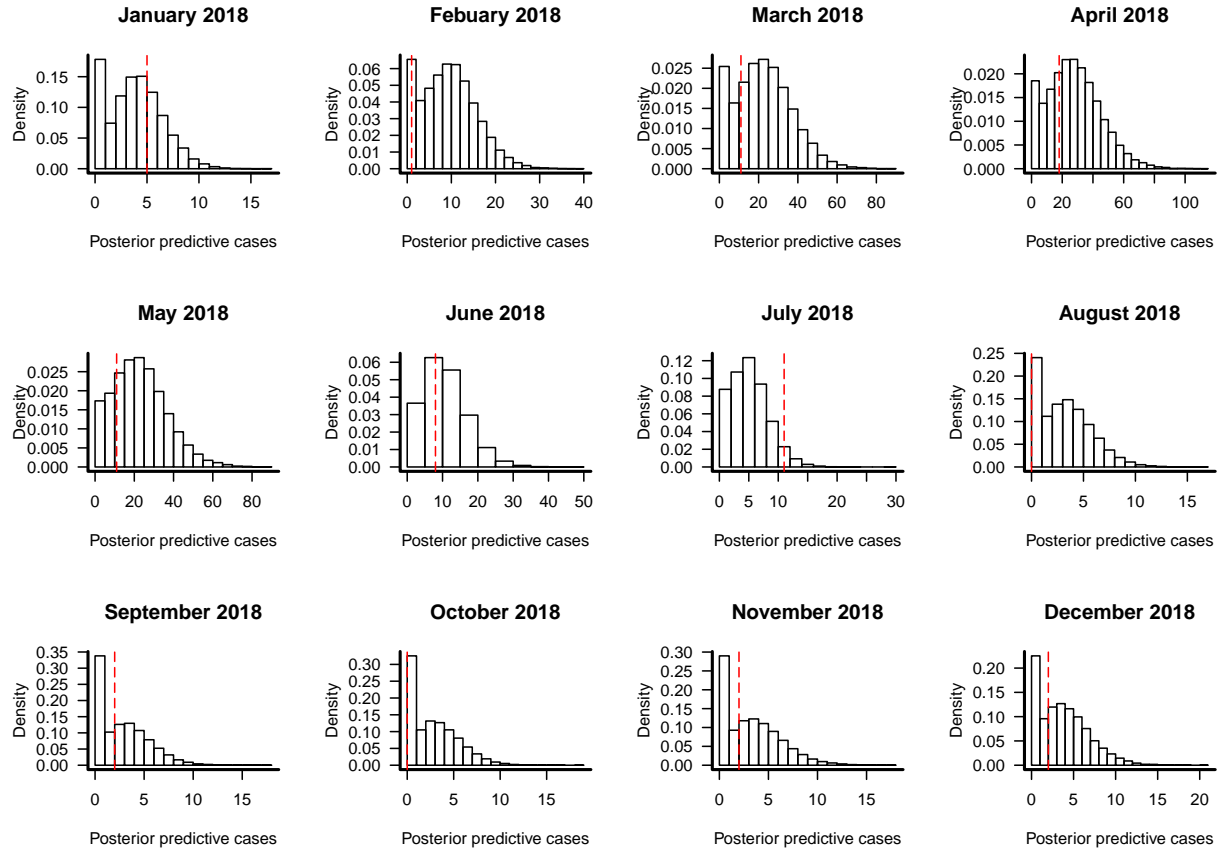


Figure 5: Histograms of the 1-12 month ahead posterior predictive distributions of the cases in the Bonsucceso district. Red dotted line represents the observed values.

Acknowledgements

This work is part of the PhD thesis of D. Douwes-Schultz under the supervision of A. M. Schmidt in the Graduate Program of Biostatistics at McGill University, Canada. Schmidt is grateful for financial support from the Natural Sciences and Engineering Research Council (NSERC) of Canada (Discovery Grant RGPIN-2017-04999).

References

Plummer, M., Best, N., Cowles, K. and Vines, K. (2006) CODA: Convergence diagnosis and output analysis for MCMC. *R News*, **6**, 7–11.

Touloupou, P., Finkenstädt, B. and Spencer, S. E. F. (2020) Scalable Bayesian inference for coupled hidden Markov and semi-Markov models. *Journal of Computational and Graphical Statistics*, **29**, 238–249.